AD-759 078

Advanced Ocean Engineering Laboratory Technical Progress Report

Scripps Institution of Oceanography

prepared for
Office of Naval Research
Advanced Research Projects Agency

MARCH 1973

Distributed By:

NTIS
National Technical Information Service
U. S. DEPARTMENT OF COMMERCE

SCRIPPS INSTITUTION OF OCEANOGRAPHY
UNIVERSITY OF CALIFORNIA, SAN DIEGO
Dr. William A. Nierenberg, Director
Principal Investigator
ADVANCED OCEAN ENGINEERING LABORATORY

Technical Progress Report

December 31, 1972

Sponsored by
ADVANCED RESEARCH PROJECTS AGENCY
ADVANCED ENGINEERING DIVISION
ARPA Order Numbers 1348, 1730 and 1607
Program Code 2N10

Administered by the OFFICE OF NAVAL RESEARCH
Contract N00014-69-A-0200-6012
Contract Effective Date: December 15, 1968
Contract Expiration Date: December 31, 1972
Total Contract Amount $3,305,602.00

SIO Reference Number 73-11

AOEL Report #38

Unclassified
Security Classification

DOCUMENT CONTROL DATA - R & D

(Security classification of title, body of abstract and indexing annotation must be entered when the overall report is classified)

1. ORIGINATING ACTIVITY (Corporate author) The Regents of the University of California University of California, San Diego La Jolla, California 92037	2a. REPORT SECURITY CLASSIFICATION Unclassified 2b. GROUP Not applicable

3. REPORT TITLE
Technical Progress Report
Advanced Ocean Engineering Laboratory

4. DESCRIPTIVE NOTES (Type of report and inclusive dates)
July 1, 1972 to December 31, 1972

5. AUTHOR(S) (First name, middle initial, last name)
Dr. Fred N. Spiess
Dr. Robert H. Stewart
Dr. Douglas L. Inman
Dr. William G. VanDorn

6. REPORT DATE March 30, 1973	7a. TOTAL NO. OF PAGES 61	7b. NO. OF REFS 12
8a. CONTRACT OR GRANT NO. N00014-69-A-0200-6012 b. PROJECT NO c. d.	9a. ORIGINATOR'S REPORT NUMBER(S) SIO Reference No. 73-11 9b. OTHER REPORT NO(S) (Any other numbers that may be assigned this report) AOEL Report No. 38	

10. DISTRIBUTION STATEMENT
Distribution of this document is unlimited.

11. SUPPLEMENTARY NOTES	12. SPONSORING MILITARY ACTIVITY Advanced Research Projects Agency c/o Office of Naval Research Arlington, Virginia 22217

13. ABSTRACT

This semi-annual report reflects the technical status of projects conducted within the Advanced Ocean Engineering Laboratory at the Scripps Institution of Oceanography. These projects are: (1) Stable Floating Platform - to conceive, design, build and demonstrate the feasibility of large stable floating platforms in the open sea. (2) Electromagnetic Roughness of the Ocean Surface - utilization of radio signals scattered from the sea surface to determine the directional spectrum of ocean waves. (3) Advanced Studies in Nearshore Engineering - field studies of the water-sediment interface under wave action in and near the breaker zone/ and laboratory investigation of the velocity field of breaking waves. (4) Wave Breaking In Deep Water - a projected two-year laboratory and field investigation of the factors controlling the breaking of mixed-frequency wave systems in deep water.

14 KEY WORDS	LINK A		LINK B		LINK C	
	ROLE	WT	ROLE	WT	ROLE	WT
Advanced Ocean Engineering						
Stable Floating Platform						
Advisory Committee (Tachmindji) Report						
New Concept						
Major Module						
Satellite Leg						
Coupling						
Instrumentation						
Electromagnetic Roughness of the Ocean Surface						
Bragg Scattered						
Range Doppler Spectrum						
Directional Antenna						
Hawaiian Bistatic Experiment						
LORAN A Radio Signal						
Wave Buoy						
Wake Island Synthetic Aperature Experiment						
Advanced Studies In Nearshore Engineering						
Phase Dependent Roughness Element						
Wave Breaking In Deep Water						
Convergent Breaking						
Wave Profiles						
Particle Velocities						
Particle Acceleration						
Phase Velocities						
Energy Budget						

Disclaimer

The views and conclusions contained in this document are those of the authors and should not be interpreted as necessarily representing the official policies, either expressed or implied, of the Advanced Research Projects Agency or the U. S. Government.

ADVANCED OCEAN ENGINEERING LABORATORY

TECHNICAL PROGRESS REPORT

Table of Contents

Part I

STABLE FLOATING PLATFORM

Principal Investigator
Dr. Fred N. Spiess
Phone (714) 453-2000, Extension 2476

ADVANCED OCEAN ENGINEERING LABORATORY

Sponsored by

ADVANCED RESEARCH PROJECTS AGENCY

ADVANCED ENGINEERING DIVISION

ONR Contract N00014-69-A-0200-6012

V

Part I

STABLE FLOATING PLATFORM

Table of Contents

List of Figures

I. Project Summary

During the six months ending December 31, 1972 the SIO Stable Floating Platform project has enjoyed significant progress in 4 areas:

First, a report has been submitted separately in response to comments (including questions and recommendations) by the Stable Floating Platform Advisory Committee convened at IDA in November 1971 and directed by Mr. Alexander J. Tachmindji. It provides a variety of information on catamaran modules. Excerpts are contained in this report.

Second, a new concept was submitted in August. It features a major module and satellite legs complex that can be expanded to extremely large size, for example, an airfield. An SIO proposal has been approved and funded by ARPA to investigate the new concept, including 1/8th scale major module and satellite leg construction and tests at sea.

Third, successful coupling and instrumentation sea tests of the two 1/8th scale catamaran modules were conducted at sea in July and subsequently in September 1972.

Fourth, the instrumentation package, described in the previous report has proved feasible. Affirmation of the total package with the computer interfaced is an objective for the final 1/8th scale catamaran module coupling tests in January 1973.

II. Advisory Committee Report

Reference A forwarded the Advisory Committee Report to Mr. Alexander Tachmindji of ARPA. Three of the eighteen comments (9 specific and 9 general comments) could not be fully answered at the time of the report. Two pertaining to slamming will be reported on in detail after final 1/8th scale catamaran module coupling tests at sea in January 1973. The other pertaining to use of lightweight concrete will be reported in full after completion of an "in sea water" adsorption test program being performed by Naval Construction and Engineering Laboratory (NCEL) at Port Hueneme, California. Late completion of the first phase "in air" tests by Smith-Emery Co. of Los Angeles, California and NCEL test equipment procurement problems precluded meeting an original planned completion date of November 1972.

Of the fifteen Advisory Committee comments fully addressed, a number were combined to avoid needless repetition in the report. One comment addresses the subject of force/motion

parameters as a function of the number of modules before finalizing design of linkage and modules. Actually, as early as 1969 SIO efforts included parametric studies of platforms extensive in size. During this six months, SIO efforts included completion of the Seadrome analysis by Consultant George Morgan (referred to in the last report) who made a great deal of sense out of a mass of data. Currently Consultant L. R. Glosten is conducting a parametric analysis of the new concept to determine optimum platform weight, platform costs, leg structure, and submerged coupling structure as functions of forces/moments and leg spacing. Additionally, a local IBM 1130 Fortran program and computer programs developed by Consultant George Morgan are being examined for possible application.

Coupling (linkage) of modules was the subject of four comments and will be discussed in detail in Section V below.

Comments on possible limitation of forty foot full scale design clearances for major modules were considered by SIO. Future designs will have a 50 foot air gap (free board). Also a prior consultant study initiated by SIO in 1969 examined storm/high wave occurrence in various areas of the world. This would be an important consideration for planning sustained operations in any given area.

Limited payload of the SFP catamaran design was discussed. The parametric study being conducted by Consultant Glosten should determine horizontal and vertical payload and other parameters in terms of a large working platform.

A comment by the Advisory Committee notes that drilling platforms obtain motion stability by increasing the virtual mass of entrained water for each leg, a capability not possible in a FLIP-type leg. Heave data for five platforms examined by Consultant Morgan indicates that none has stability comparable to FLIP (Figure 1). Additionally, in a multistructure with cross ties between legs near the bottom, there is significant opportunity to build deep cross decking which could entrain water in a much more effective manner than with a shallow draft structure.

Several comments relative to use of concrete will be appropriate only if a decision is made to use concrete in future leg construction. These comments will be considered if such a decision is made. The lightweight concrete water absorption tests mentioned above were already underway when steel was chosen as the structural material; therefore, they were continued. The results should be of benefit to general marine concrete technology regardless of whether concrete is to be used in future SFP design and construction.

In general, although the Committee comments were directed towards the catamaran modules, most are equally applicable to any Stable Floating Platform. SIO will continue to use the valuable guidance provided by the Advisory Committee whenever applicable to the current on-going program.

III. New Concept

Reference B forwarded a detailed study to ARPA which described a new concept which supersedes the "catamaran modules" concept. It responds to the change in policy requirements expressed by ARPA in late calendar year 1971. It will offer a more versatile and practical design in terms of expansion from a single module to a large "airfield" type platform.

The new concept can be directly generalized to large areas and yet draws upon most of our previous analytical and model work relating to platform motions and the forces exerted by the sea. Basically the system utilizes a major module, of the sort shown in Figure 2. This craft can operate in either a horizontal or vertical mode and can carry a deck load consisting of a number of FLIP-like columns which would be the large platform supporting elements. These would be loaded on deck in port, and the entire rig (looking like a conventional large seagoing barge with deckload) would be towed to the assembly area. Once on station the major module would flip, with its deck load still attached and then, once in the vertical, would release the individual columns to be pulled away one by one by the tug into position for coupling. The several legs (and the major module) would be coupled into a single rigid structure (interconnected top and bottom) which would then be mated to other similar subgroups to form the entire platform, which could then be decked over to provide the desired landing area. The major module could, alternatively, be returned to port to bring back more satellite units, to allow for optimizing the mix of columns and the major modules in the final platform. One plausible configuration would be to carry five legs as a single load and put these together with their parent major module on a square grid with 200-ft leg spacing and enough deck overhang to provide a 400 by 500-ft area. The 100-ft overhang on two opposite sides would be feasible when additional modules were connected at that point. One effective overall geometry would be a cross configuration 6000-ft tip to tip (Figure 3) with each arm 500-ft wide made by assembling 29 of these subgrops. The cross shape in these dimensions would provide for landing and takeoff of C130-type aircraft with arbitrary orientation of the platform relative to the wind.

Reference C forwarded an SIO proposal to ARPA to define and investigate the feasibility of the major module/satellite leg platform system with a primary objective of a structure that can expand to a large, column stabilized platform of airfield size. The proposal has been approved by ARPA and funds transferred to the Office of Naval Research.

SIO has accomplished the following in implementation of the new program:

1. Approved a preliminary design for the major module.

2. Constructed a 1/100th scale major module model.

3. Tested 1/100th scale major module model in SIO Hydraulic Laboratory Wave Channel in horizontal, vertical and flipping sequences. Results were highly encouraging although some tests will be repeated after the wave generator and channel are overhauled.

4. A preliminary parametric analysis has been submitted by Consultant L. Glosten. After some realignment of objectives, he has commenced work on a final version (see 2. below).

Currently, the following actions are underway:

1. Final builders plans and specifications for 1/8th scale major module construction are being completed.

2. Final parametric analysis is being developed.

3. Preliminary leg/strut design is being developed subject to conclusions drawn from 2. above.

IV. Coupling

The IDA Advisory Committee (section II above) made several comments that directly related to coupling. In developing the coupling system, SIO actually has gone beyond the Committee's recommendations. The 1/8th scale modules are being tied together rigidly at both the top and bottom. The bottom coupling connections are to eliminate heave between modules. The upper deck (or superstructure) and bottom coupling connections prevent relative horizontal motions. Since the upper connection therefore need not withstand bending moments, the linkage can be much lighter. It presently is planned to use a similar approach in the major module/satellite leg efforts.

Actual operation at sea of a workable coupling system for the 1/8th scale catamaran modules proved to be a major effort during second half, calendar year 1972. Successful coupling/uncoupling was effected initially during a two day at-sea period in July 1972. During the operations, the equivalent of up to sea state 5 was experienced.

In September, an improved coupling design was employed. It incorporated lessons learned from July tests. For example, wire cable rigging was substituted for nylon line which caused some earlier problems. The sea state experienced was the equivalent of force 4. However, heavy swells, confused as to size, direction, and period, actually created much more pitch and surge during coupling/uncoupling than during the July trials. Overall, successful coupling/uncoupling was effected with significant wave heights up to 2.5 feet (full scale height of 20 feet) experienced.

One more final sea trial is planned for the catamaran modules in the early calendar 1973 time frame. A primary objective will be operational testing of an instrument package that includes a computer for data logging and reduction (section V below). Additionally, valuable coupling, uncoupling experience will be gained and force/motion data will be collected.

Figure 4 gives actual dimensions for 1/8th scale modules. The couple distance, when coupling is effected between appropriate module legs, is about 14.8 feet from leg axis to leg axis. Of considerable significance is that this translates to approximately 118 feet for a full scale model. The minimum horizontal distance between adjacent superstructure top edges is 37". This translates to about 24 feet.

Detailed discussion of coupling design (Figures 5 and 6) and operation follows:

1. Lower Linkage

The lower linkage is accomplished through two ball-and-socket joints, one on each side of the module, so that when coupled it is equivalent to a hinged joint, thereby removing five of the six relative degrees of freedom.

In the current coupling concept, the modules are drawn together and held together by 3/16" diameter stainless steel cables. On the female module the cable goes into the funnel through the inside of the 4x4 square-section strut, and over sheaves up to the superstructure where the cable on each side is taken up by winches rated at 2000 lbs.

On the male module, the upper ends are connected to load cells and tensionmeters for data recording and trial read-out of cable tensions. To alleviate line handling and retrieval problems, the cable on the male module is made to form a continuous loop (Figure 6). This allows the point of linkage between the cables to be pulled from top to bottom or vice versa. The modules can be then connected, disconnected and connected again without having to flip to the horizontal to re-rig any lines.

The linkage at full scale will be some 250 feet below the water surface, where it would be extremely difficult to correct any malfunction. Therefore, latches or locks were eliminated, and the entire system was made as simple as possible.

In actual operation, the lower linkage performed remarkably well with no operational difficulties. The cable loads remained low until the hook-up was completed with the cables post-tensioned to about 1000 pounds.

2. Upper Linkage

In the original design, the upper linkage was a single tie rod with ball joints at either end, to eliminate the sixth degree of freedom. However, in the July sea trials it was found that there was sufficient flexure in the lower connection to allow relative side to side motions at the top, as well as fore-aft motion. To eliminate the sideways relative motion, the upper linkage was changed to the two diagonal strut arrangement.

The upper linkage, though successful, generated more operational difficulties than the lower. This was due to the much greater relative surge between modules at the surface. Inflated rubber bumpers were used to absorb impact loads between supersturctures during coupling. In retrospect, it is thought that this probably created more difficulties by acting as a spring which, when coupled with the flexible nylon tether line used to pull the supersturctures together, set up a resonant motion between modules. A stiffer cushion and steel instead of nylon lines will be used in the January sea trials.

3. General

The catamaran coupling design made the coupled modules into a structurally redundant system, for which it is difficult to translate theoretical hydrodynamic

forces into strut loads for comparison of theoretical and actual loads. However, it is easy to calculate total imposed forces from the measured strut loads. These results then can be compared to the theoretical hydrodynamic loads. This will be reported in more detail after analysis of January trials.

Catamaran coupling operations to date have been limited to mating of the two 1/8th scale modules. In the new concept and the programmed calendar 1973 objectives, an 1/8th scale major module and two legs will be coupled. The geometry and coupling distances will be determined from the previously mentioned parametric analysis being conducted. Not only will a primary on going objective be to solve the problem of first mating a major module/satellite leg platform complex, but also the complexities of marrying small complexes together to form a large (e.g., airfield) operational platform will be considered. The stability both of the smaller platform and larger complex also will be studied.

The extent to which the problem can be investigated encompassing the mating of individual stable platform units to form a small complex, those to form larger ones, will be determined by funding. Current anticipated funding through calendar year 1973 will not permit more than study of the problem.

The very successful coupling experience in July and September 1972 together with anticipated additional experience in January 1973 will undoubtedly contribute to resolution of major module/satellite leg coupling design and implementation at sea. The results to date clearly demonstrate that coupling is feasible even under adverse sea conditions.

V. Instrumentation

A partial instrumentation package consisting only of a wave meter and the vertical channel of an accelerometer was tested during July coupling tests at sea. In September a larger package was utilized that was limited primarily by the simultaneous recording capability of a seven channel magnetic tape recorder and an eight channel paper strip recorder. Instruments were mounted generally as shown in Figure 7.

Although cost, time and design considerations injected some limitations and problems, the feasibility of the instrument package comparing force/motion/sea state data was confirmed.

As the year (1972) ends, the PDP-8E computer system has been interfaced into the instrumentation system. A two month delay in delivery of the computer will limit the processing capability for the final 1/8th catamaran module tests in early calendar year 1973 but a full data collection capability has been programmed. With a full 20 channel simultaneous computer recording capability backed up by a 14 channel tape recorder, the instrument package will give a versatility and redundancy that will greatly enhance the real time force/motion study capability. When full processing ability is realized together with a capability to analyze immediately after each recording run, the instrument package will enjoy its full potential.

VI. Future Plans

The following minimum objectives are planned for the first half of calendar year 1973 (January to June inclusive):

A. Final instrumentation trials for the two 1/8th scale catamaran modules.

B. Full processing, analysis and evaluation of data collected in paragraph A above.

C. Programming for processing/analysis capability with PDP-8E system.

D. Construction and testing of 1/8th scale major module.

E. Finalization of design and construction of two 1/8th scale satellite legs and coupling members to form a triangular platform with a major module.

F. Testing and evaluation of 1/100th scale major module/satellite leg complex in SIO wave channel.

VII. References

A. University of California, SIO AOEL Serial #684 of December 18, 1972

B. University of California, SIO AOEL Serial #634 of 25 August 1972 (concept)

C. University of California, SIO AOEL Serial #654 of 5 October 1972 (enclosure is UCSD Request for Extramural Support #5547 of 10/2/72)

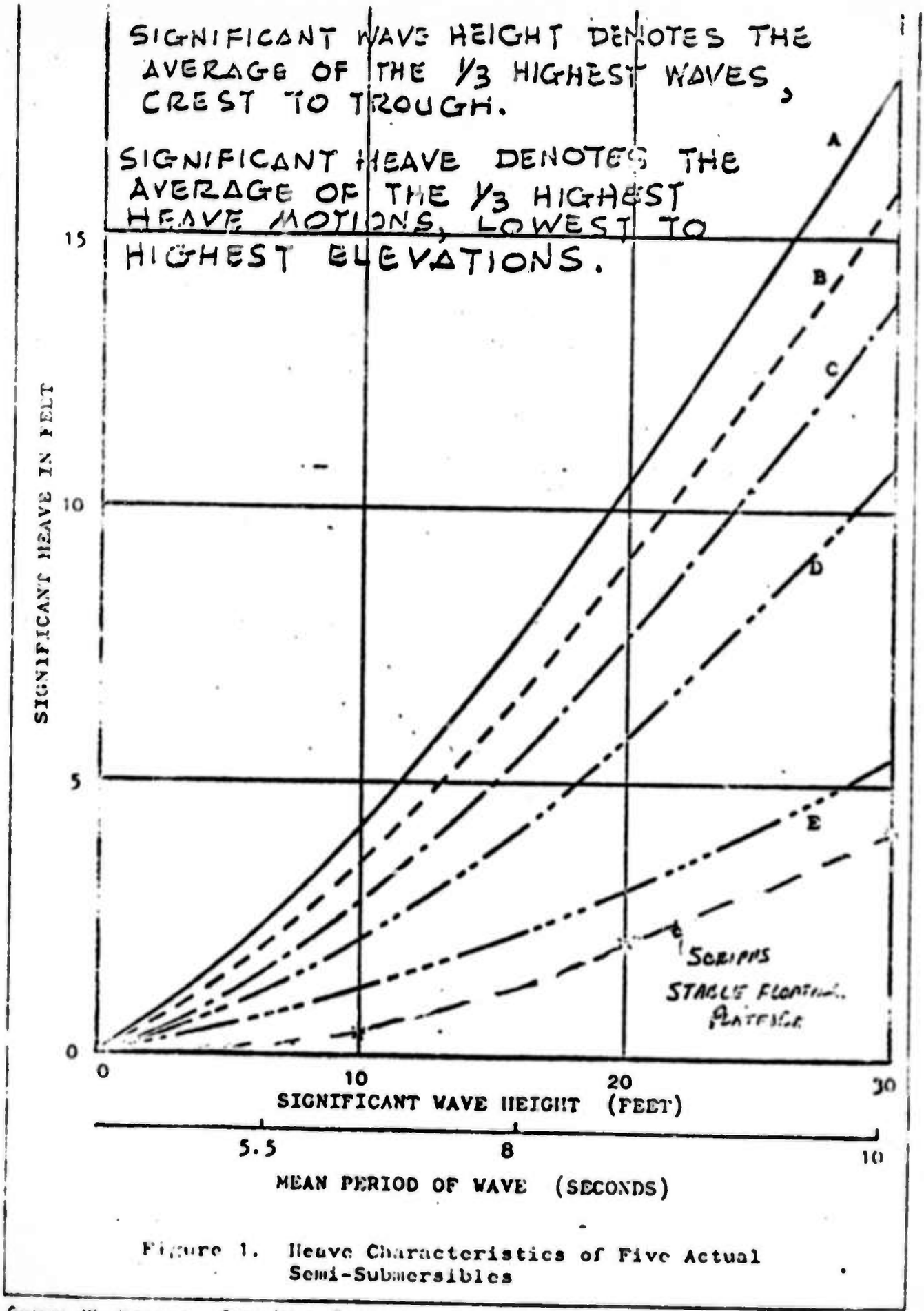

Figure 1. Heave Characteristics of Five Actual Semi-Submersibles

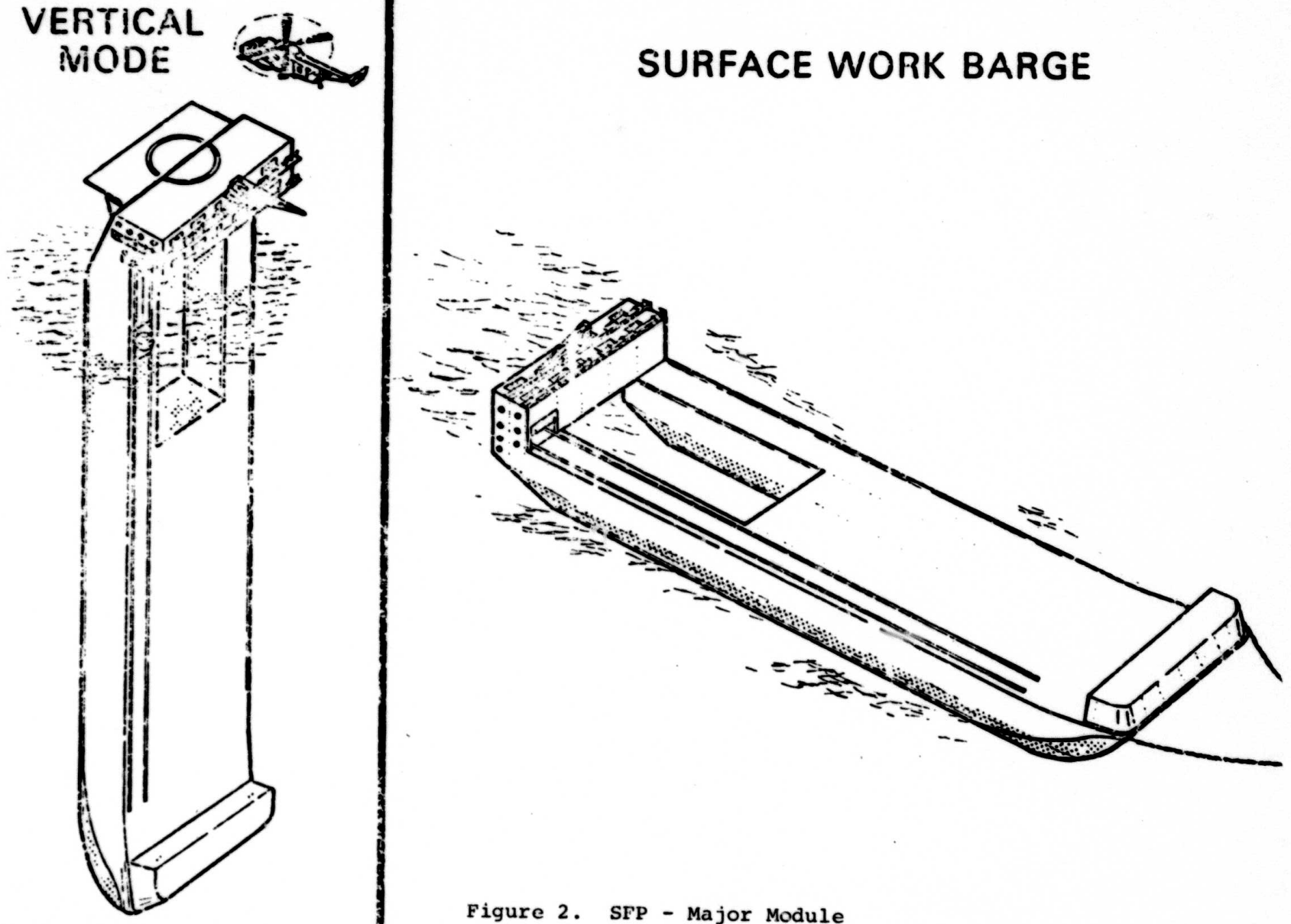

Figure 2. SFP - Major Module

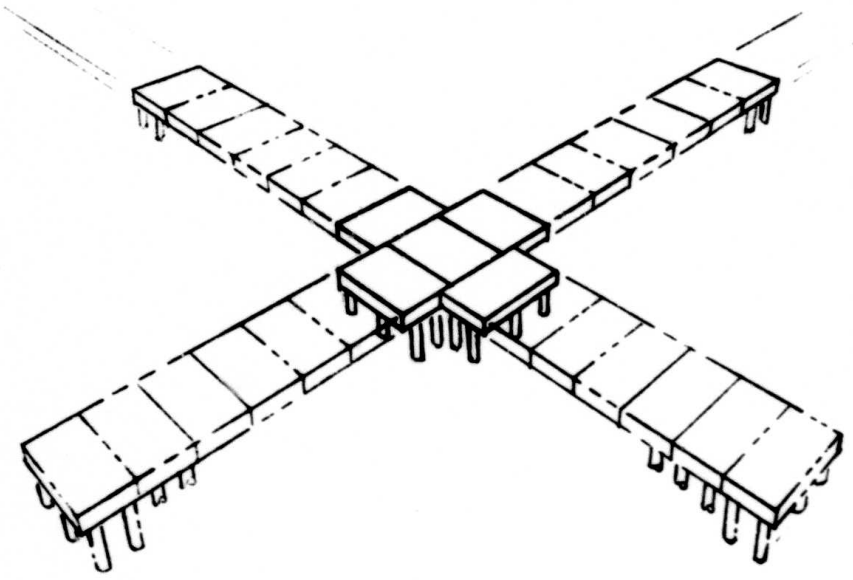

Figure 3. Example of Possible Large Platform Configuration

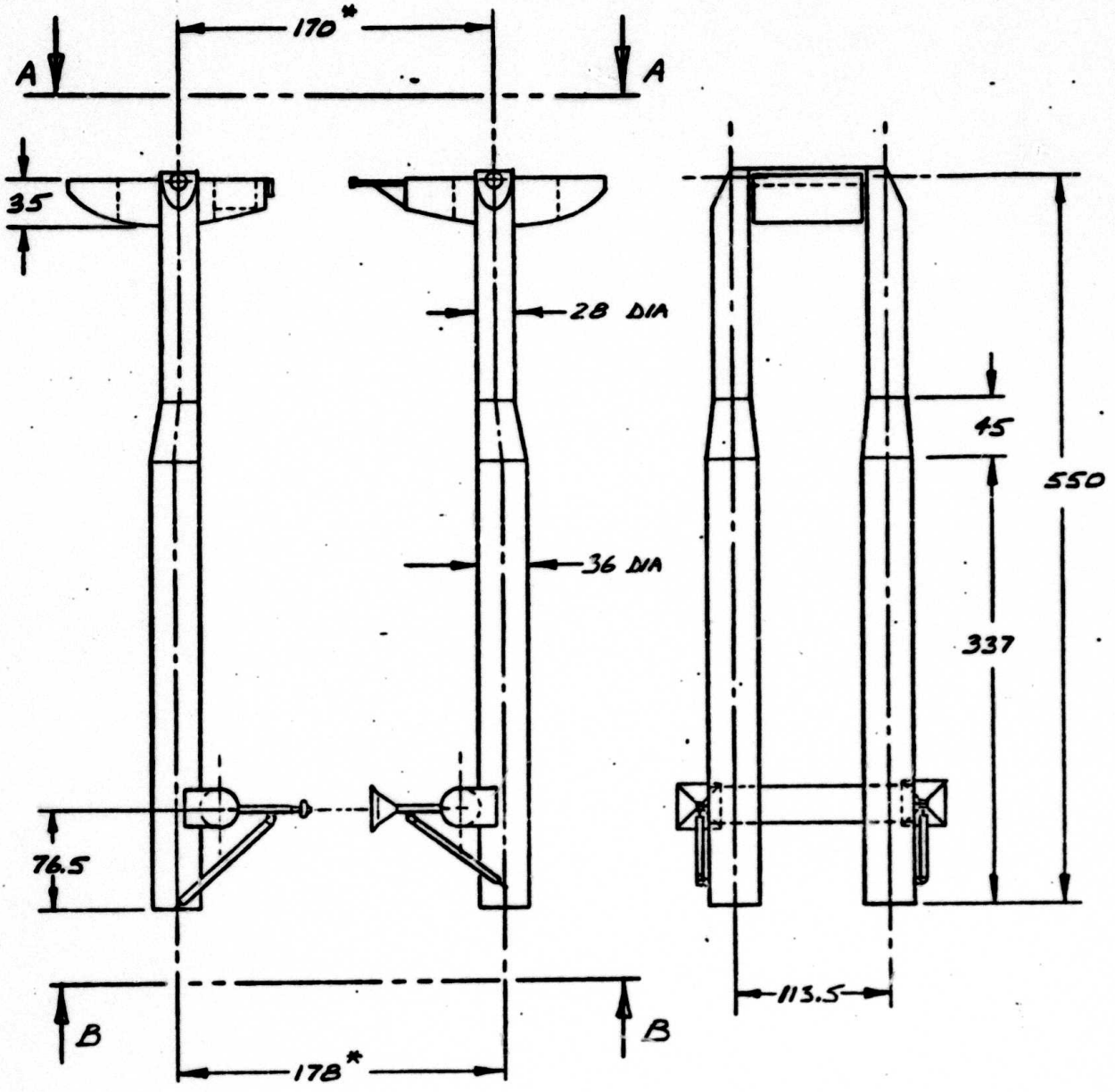

Figure 4. 1/8 scale catamaran model configuration
All dimensions in inches.
* (in mated condition)

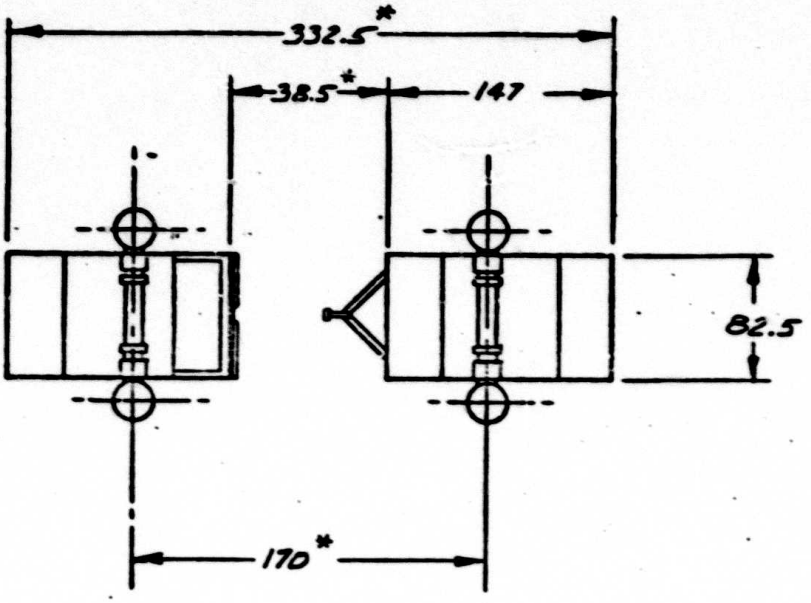

VIEW A-A (TOP VIEW)

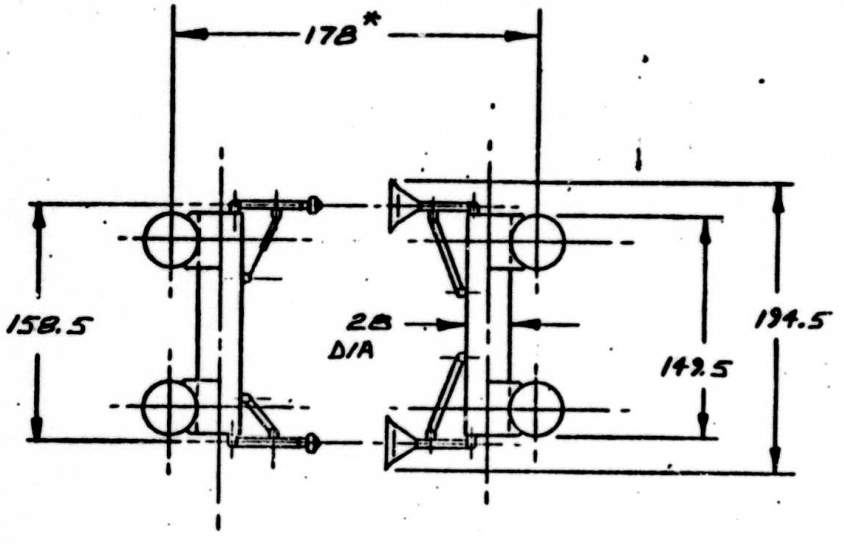

VIEW B-B (BOTTOM VIEW)

Figure 5. 1/8 scale catamaran model configuration Top-Bottom
All dimensions in inches
* (in mated condition)

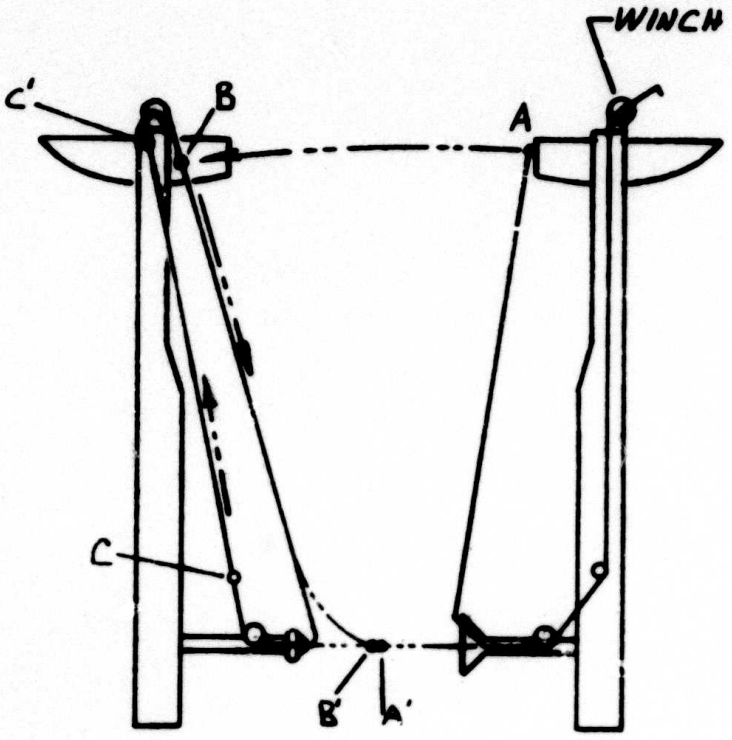

Figure 6.
Coupling Procedure

1. Attach cable end A to ring B
2. Pull ring B to bottom position B'
3. Attach ring C to upper leg structure
4. Take up slack at winch
5. Reverse procedure for uncoupling

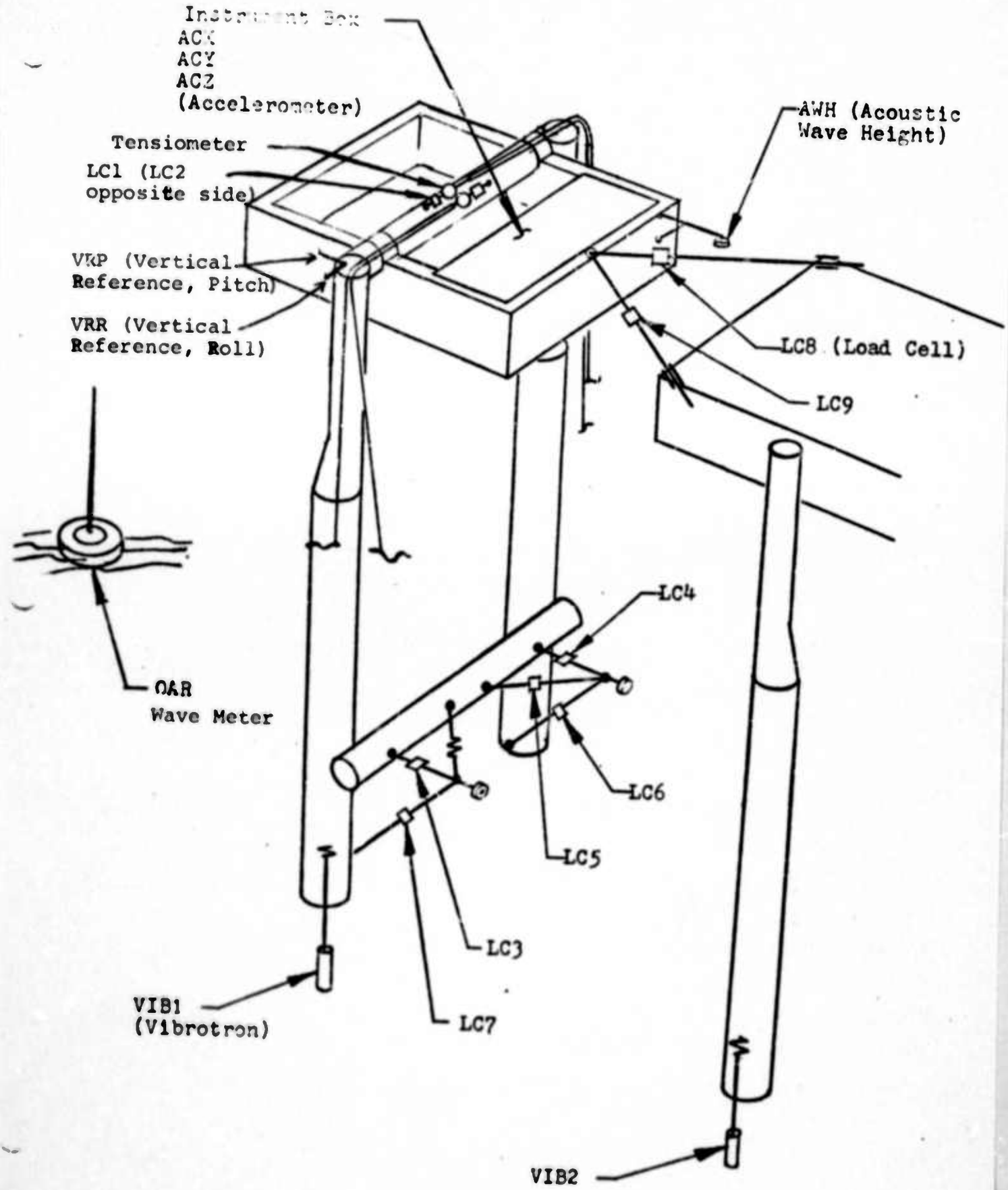

Figure 7. Instrumentation Package

Part II

ELECTROMAGNETIC ROUGHNESS OF THE OCEAN SURFACE

Co-Principal Investigators
Dr. Walter H. Munk
Phone (714) 453-2000, Extension 1741
Dr. Robert H. Stewart
Phone (714) 453-2000, Extension 2476

ADVANCED OCEAN ENGINEERING LABORATORY

Sponsored by

ADVANCED RESEARCH PROJECTS AGENCY

ADVANCED ENGINEERING DIVISION

ONR Contract N00014-69-A-0200-6012

Part II

ELECTROMAGNETIC ROUGHNESS OF THE OCEAN SURFACE

Table of Contents

List of Figures

I. Project Summary

The electromagnetic roughness studies are being conducted jointly by two groups, one at Stanford and one at Scripps Institution of Oceanography. The work uses HF radio waves scattered from the ocean surface to measure the statistical properties of this surface, particularly the ocean-wave directional spectrum.

The six month period covered by this report was entirely occupied with the planning and execution of two major field experiments.

The first experiment performed in September in Hawaii was designed to: 1) measure part of the directional spectrum of 7-10 s ocean waves in a homogeneous sea using a bistatic geometry and 2) accurately compare the theoretical to the observed radar cross-section of the sea surface.

The second experiment, at Wake Island in November, was designed to measure the complete, 360° directional spectrum of seven-second ocean waves in a homogeneous sea using a synthetic-aperture technique.

II. Technical Report

A. Introduction

The purpose of this contract, as stated in our proposal, is to use radio waves Bragg scattered from the sea as a tool to measure the statistical properties of the ocean surface. In particular, we are evaluating techniques for measuring the most important two-dimensional statistical property of the ocean surface, the ocean-wave directional spectrum. These techniques include situating the radar receiver and transmitter in 1) a bistatic geometry and using the range-Doppler spectrum of the scattered signal to determine the wave directions; 2) a monostatic geometry which uses a directional antenna to obtain the same information; and 3) a monostatic geometry with a moving receiver, where the motion of the receiver is used to synthesize a directional antenna.

Our work to date has been described in three previous semi-annual reports, but can be briefly summarized. During the first year of the contract, a portable, low-power LORAN A receiver; an antenna for the receiver; and a pitch-and-roll wave measuring buoy were designed and built. In September of that year, existing LORAN A radio signals (at 1.85 MHz) were received by the receiver in a bistatic-geometry experiment to measure the directional spectrum of a fully-

developed homogeneous sea. The receiver was placed on board a small ship located at a point north of the Hawaiian Islands such that the baselines from the receiver to the Hawaiian LORAN transmitters were at right angles, and aligned perpendicular and parallel to the wind. This geometry was chosen to give maximum coverage of the ocean-wave number spectrum. The one-dimensional ocean-wave spectrum was measured using a rented buoy since the pitch-and-roll buoy was not completed in time for this experiment. In addition, some radar data was recorded at locations on Oahu and Maui.

This year we have conducted a number of field experiments, the first of which were designed to determine the importance of higher-order scatter at higher HF radio frequencies. The experiments consisted of measuring the Doppler spectra of 30 MHz radio signals backscattered from the sea on a number of different days for various wind and wave conditions. On three of these days the ocean waves and surface currents were measured using the pitch-and-roll buoy and surface drogues. The Doppler spectra showed that at this frequency higher-order scatter is nearly as strong as the Bragg scatter and that the shape of the spectra sometimes agreed qualitatively with that predicted by theory, but that at other times it did not.

The other field experiments, at Hawaii and Wake Island, are the subject of this report.

B. Hawaiian Bistatic Experiment

The bistatic-geometry method of measuring the directional spectra of ocean waves consists of recording the range-Doppler spectrum of radio signals scattered from the sea with a receiver that is located at a considerable distance (typically 150 km) from the transmitter. If the wave field is homogeneous throughout the scattering area, then each point in this spectrum can be related to four symmetric points in the ocean-wave directional spectrum (see Teague, 1971 for a description of this mapping).

The first Hawaiian bistatic experiment was done in September 1971 using a shipborne receiver located off the coast of Hawaii, and has been described in an earlier report (ARPA Semi-Annual Report for June 30, 1972). Analysis of data recorded during this experiment showed that the additional Doppler shifts induced into the spectrum of radio signals scattered from the sea by the ship's motion, while small, seriously distort the interpretation of the data and introduce serious errors into the calculation of the ocean-wave

directional spectrum. We therefore decided to redo the experiment with a number of important changes.

The second experiment was again performed in Hawaii, but the radio receiver was located on land to eliminate Doppler shifts in the received signal due to receiver motion. This location meant that the expected symmetry of the ocean wave spectrum about the mean wind direction would not coincide with one of the axis of symmetry of the bistatic geometry as it had in the first experiment; and, therefore, the scattered radio signals had to be recorded with a steerable directional antenna array. In addition, because the receiver was on an island, the ocean-scattered radio signals coming from certain directions were attenuated by mountains on the island. The receiver site was carefully chosen so that this shielding was an asset rather than a liability.

In the following paragraphs we will describe the work involved in designing the receiving antenna array, the selection of the receiving site, the calibration of the experiment, and the conduct of the experiment.

1) Antenna Design

The interpretation of the bistatic geometry data involves associating each point in the ocean-wave directional spectrum with a point in the range-Doppler spectrum of the scattered radio signals. Unfortunately, each point in this radio spectrum comes from four different scattering areas symmetrically located about the receiver-transmitter baseline and its bisector, so a receiving antenna with a beamwidth of approximately 90° must be used to determine the relative signal strength coming from each of these symmetric areas.

An antenna of the desired beamwidth was constructed from four loop antennas. The phases of these elements were switched to form a beam which looked sequentially in four different directions (quadrants).

The four simultaneous sets of data received by each of the four antenna beams was used to solve a set of four equations to determine the scattered signal strength from each of the bistatic scattering areas. An analysis of the errors in the solution of this set of equations using simulated data plus a small amount of noise indicated that 1) the signal-to-noise ratio of the data is reduced by about 10 db; 2) the error becomes smaller as the bistatic baseline is increased; 3) the solution has a region of high error where the set of equations becomes singular; but 4) this region of high error occupies a small area in ocean-wave number

space if the antenna elements are oriented at approximately 120°-60° with respect to the bistatic baseline. The final antenna configuration used in the experiment is given in figure 1.

2) Site Selection

Considerable care was taken to select a suitable site where the attenuation of the received radio signals due to propagation over land would simplify rather than complicate the data analysis. Two geographic scales were considered in the selection process. The first concerned the selection relative to the islands and the LORAN transmitters on them; the second concerned the siting of the antenna relative to the shoreline. We will call these the macro and micro scales respectively.

The macroscale selection made use of six criteria, which were, in order of importance: the site must 1) be accessible; 2) be on the coast; 3) have a clear view of the scattering area illuminated by the transmitter; 4) view a scattering area upwind of the islands; 5) have a long transmitter-receiver baseline; and 6) have high shielding by mountains of signals coming from a 180° sector (to reduce the number of ambiguities in the data due to bistatic symmetries).

The strength of LORAN A radio signals were measured along the coasts of the Hawaiian Islands to determine the amount of shielding by mountains and to find accessible sites. A number of possible sites were selected on the basis of the first five criteria. Then the location of land and areas shielded by land were mapped from geographic coordinates to ocean wave number space. This is possible because the bistatic geometry produces a one-to-one map from geographic space to range-Doppler space to ocean wave-number space (neglecting symmetries). The last criterion was then used to make the final selection of a site.

The measurements of signal strength near the shore indicated that the fringing RF field at the ocean-land interface in the Hawaiian Islands (due to reflection of RF energy from the change in conductivity at this interface) was important, and must be accounted for. Further measurements showed that the distortion of the direction of arrival are small enough to be neglected when the receiving antenna is located a few hundred feet from the shoreline. This defined the microscale site selection criterion.

The site finally chosen for the receiving antenna was on the north coast of Hawaii 30 km south of Hilo at Waiakahula, a few hundred feet from the shore, and about 30 feet above sea level. The baseline from the transmitter at Upolu on the N.W. tip of Hawaii to the receiver was 135 km.

A map of the Hawaiian Islands showing the receiving site is figure 2. A mapping of this site into the ocean-wave directional spectrum space is figure 3. This latter figure shows that the site has a clear view of waves coming from 20° west of north to 10° south of east, and a maximum amount of attenuation for waves coming from the opposite direction.

3) Calibration

One of the goals for the experiment was to accurately measure the radar cross-section of the sea. This required that we measure both the strength of the incident radio field in the scattering region, and accurately calibrate the radar receiver and antenna.

The relative LORAN A field strength as a function of position on the ocean was measured by a receiver on board the R/V HOLOKAI. Field strength measurements were made every fifteen minutes while the ship went from its base in Oahu to Hilo and back. The ship's tracks, given in figure 2, were chosen to investigate the effects of shielding by a large mountain and by the local topography at the Upolu Point LORAN station. The outbound course was radially away from the LORAN station at Makahuena Point, Kauai and downrange of the mountains on Oahu, so the series of measurements on this track measured the field behind a mountain as a function of range. The series of zigzag tracks near Hawaii were chosen to investigate both the radial and azimuthal dependence of the field around the Upolo Point transmitter. A long section of the return track was the same as the outbound track so we could estimate repeatability of the measurements.

The azimuthal dependence of the receiving antenna was calibrated by carrying a low-power radio beacon along an arc with a radius of a three kilometers centered on the antenna. The antenna beam pattern was very similar to the expected pattern and was repeatable.

4) Experimental Procedure

The experiment was conducted from 13-22 September 1972. The first three days were used to measure the LORAN field strength in the scattering area and to calibrate the receiving array. In addition, the array was recalibrated on 18

September. The scattered LORAN signals were recorded for four days while the pitch-and-roll buoy was operating about 25 km offshore of Hilo in the region marked in figure 2. Additional LORAN field strength measurements were made on the last two days.

The trade winds were blowing at a nearly constant speed and direction during the period that data was collected. The wind speed as measured by the ship, when the wave buoy was deployed, was 4-6 m/sec from the east, but this value was almost certainly influenced by the presence of the island. Surface wind charts issued by the weather bureau in Honolulu showed parallel isobars extending 1500 km to the East (upwind) and north of the islands, with winds of 7-10 m/sec in this region. This isobar pattern remained essentially unchanged from the 16th to the 21st of September, so the wave field was expected to be in equilibrium with the wind on days data was collected.

The scattered LORAN A radio data and the wave-buoy data, together with the calibrations, will enable us to calculate the absolute radar cross-section of the sea for 2 MHz radio waves, and will provide bistatic measurements of a portion of the ocean-wave directional spectrum.

C. Wake Island Synthetic Aperture Experiment

The synthetic aperture technique is one that uses motion of a radar set to synthesize an antenna having a large aperture and thus high angular resolution. This technique was used in an experiment to measure the directional distribution of ocean wave energy at a single frequency in the wave spectrum of a homogeneous sea in equilibrium with a constant, homogeneous wind field. In the following paragraphs we will describe the theory for the experiment, the equipment used for the measurements, and the experiment at Wake Island.

1) Theory

The simplest technique to measure the ocean-wave directional spectrum, $\psi(k,\phi)$, uses a transmitter and reciever at the same location (monostatic geometry) together with a very directional antenna in the middle of an area 20-30 km on a side where the ocean wave field is homogeneous. Only backscattered signals from ocean waves travelling radially toward and away from the radar will be observed, and the antenna is used to determine the strength of the scattered signal as a function of azimuth ϕ and thus the variation of ψ with ϕ. By changing the radar frequency, the radio wavenumber k_i is changed, and the dependence of ψ on k is obtained.

If only a single radio frequency is used, $\psi(k,\phi)$ will be measured at a single, fixed value of k, given by the Bragg backscatter equations. These are

$$\vec{k} = -2\vec{k}_i \qquad f_o = f \qquad (1)$$

where f_o is the Doppler frequency of the scattered radio wave, and f is the frequency of the ocean wave having a wavenumber k.

This technique has one serious disadvantage; it requires a very large receiving antenna to observe commonly occurring ocean waves. This can be illustrated by a simple example. The peak in the ocean-wave spectrum is often around 0.14 Hz. From the wave dispersion relation we can calculate that a wave at this frequency has a wavelength $L = 2\pi/k_o \approx 80$ m; and from the Bragg conditions (1), a radio wave must be 160 m long to be backscattered from it. Now a broadside antenna having an azimuthal resolution of $\Delta\phi = 10°$ at this wavelength must be approximately $51/\Delta\phi$ wavelengths long, or nearly 1 km. Such a large antenna is not convenient, and less direct techniques have been sought.

If the radio set is mounted on a moving vehicle, then the motion of the vehicle can be used to synthesize a narrow beamwidth antenna. Consider a radar moving on the ocean surface towards ϕ_s with speed v_s (figure 4). Radar signals scattered from a patch of ocean with coordinate ϕ_w will be received with a frequency shift

$$\Delta f = 2v_s f_r/c_r \cos(\phi_s - \phi_w) \pm f_o \qquad (2)$$

where f_r is the radar frequency, c_r is the velocity of light, and the $\pm$ results from ocean waves travelling toward or away from the radar. Thus, ignoring ambiguities, each Δf can be associated with a particular ϕ, and, through the Bragg condition, to an ocean wave direction. If v_s is less than the wave phase velocity, c, then the inversion of (2) has only one ambiguity which can be easily resolved by using an asymetrical receiving antenna.

The angular resolution of the synthesized antenna is the same as that of an antenna as long as the path traversed by the moving radar, and is independent of the radar velocity, provided the velocity is uniform. If the velocity is not uniform, but well known, the simple, unfocused synthetic-aperture theory given here can be modified to account for the motion. Unknown velocity components will degrade the directional resolution of the synthesized antenna.

It is important to note that a measurement of $\psi(k,\phi)$ using this technique requires a homogeneous patch of ocean because each different ϕ is related to a different scattering area located along a circle centered at the radar.

2) Equipment

The radio set used for this experiment is a pulsed-Doppler radar; that is, a radar which transmits a train of pulsed radio waves whose phase is coherent from pulse to pulse. The pulses enable the radar to descriminate in range; the coherence of the pulses allows the Doppler spectrum, and thus, f, to be calculated at each range.

Because it is convenient, we have used LORAN A transmissions as a source of coherent, high-power, radio signals. These are at 1.85 MHz; have a pulse length of 100 waves (50 μsec), so $|k|$ is known to better than 1%. This signal is typically received for coherence times of 1000 s, so f is known to 1 mHz; and the high power of the LORAN transmissions allows us to receive signals from scattering areas as far as 300 km away.

To remove the right-left ambiguity of the synthesized antenna we used a cardoid antenna as the basic receiving element. The main lobe of the antenna was pointed at right angles to the direction of motion, and was switched alternately to the right and left while the vehicle was moving. The signal from the two scattering areas giving the same Doppler frequency are thus received with two different weights. This data is used to solve a pair of equations to obtain the signal from each scattering area. The solution to this pair of equations is very sensitive to errors in the data when the scattering areas are nearly straight ahead or behind the direction of motion, so two nearly orthogonal paths must be used to obtain unambiguous 360° directional measurements.

In July 1972 we conducted an experiment to determine the usefulness of the synthetic aperture technique. A LORAN A station was used, one next to a straight section of coast near Scripps Institution of Oceanography. A receiver was mounted in a car and repeatedly driven along a straight two-mile-long section of highway near the transmitter and parallel to the coast. Data from this experiment showed strong return from stationary objects which could be correlated with large hills and offshore islands, as well as scatter from the sea in the correct frequency bands.

3) Wake Island Experiment

In November 1972 this technique was used to measure the directional spectrum of seven-second ocean waves in a homogeneous trade wind region. This experiment used the LORAN A transmitter on Wake Island and a receiver on a vehicle driven on the runway and taxiways of the island. The right-left ambiguity was resolved by using the switched receiving antenna which looked alternately to the right and left of the vehicle's path. This island, shown in figure 5, was chosen because it is very small, has a long runway, and is in the middle of the Pacific trade wind region remote from any other land, and has a LORAN transmitter.

Data were collected for nine days under nearly ideal meteorological conditions. The wind speed increased slowly from 5-15 m/sec, but was constant within ±10% for many 12 hour periods during this time. At the end of this period Typhoon Ruby passed near the island, and peak winds of 20 m/sec were recorded at the island, and up to 50 m/sec at the storm's center.

The data consisted of almost 200 repeated synthetic aperture measurements over nearly orthogonal paths of 2.7 and 1.0 km length, and many hours of data with the receiver stationary. In addition, ocean waves were measured upwind of the island using a pitch-and-roll buoy on two different days.

We are now in the midst of analysing this data. One of our first Doppler spectra obtained with a stationary receiver is illustrated by figure 6. As has been mentioned earlier, this spectrum has two sharp lines at the frequencies predicted by the Bragg theory, and these lines extend 1000 times above any other features in the spectrum. These sharp clean lines have sidebands which extend nearly 100 times above the noise level; and are probably due to higher order scatter. Furthermore, the sideband at -0.22 Hz is very much like the ideal sideband predicted by the second-order theory. This is the first time sidebands have been observed at such low radio frequencies.

Our first directional spectra show features to a resolution of 10°, and spectra measured on orthogonal paths are identical. Although the bulk of the data processing remains unfinished, we have processed enough to know that the data will provide for the first time directional spectra of seven-second ocean waves to a resolution of greater than 10° for various wind conditions.

The spectra obtained by this technique have an order of magnitude improvement in angular resolution over previous measurements, are of high signal-to-noise ratio, and were recorded under nearly ideal meteorological conditions. Because the weather conditions were so favorable, we took advantage of the opportunity and collected as much data as possible. The amount of data was more than we expected in planning the experiment, and considerably increased the scope of the experiment, but the additional data will provide important information about the dependence of the directional spectrum on wind speed.

III. References

Teague, Calvin C. 1971 Bistatic-radar techniques for observing long-wavelength directional ocean-wave spectra. IEEE Trans. on Geoscience Electronics, GE-9, 211-215.

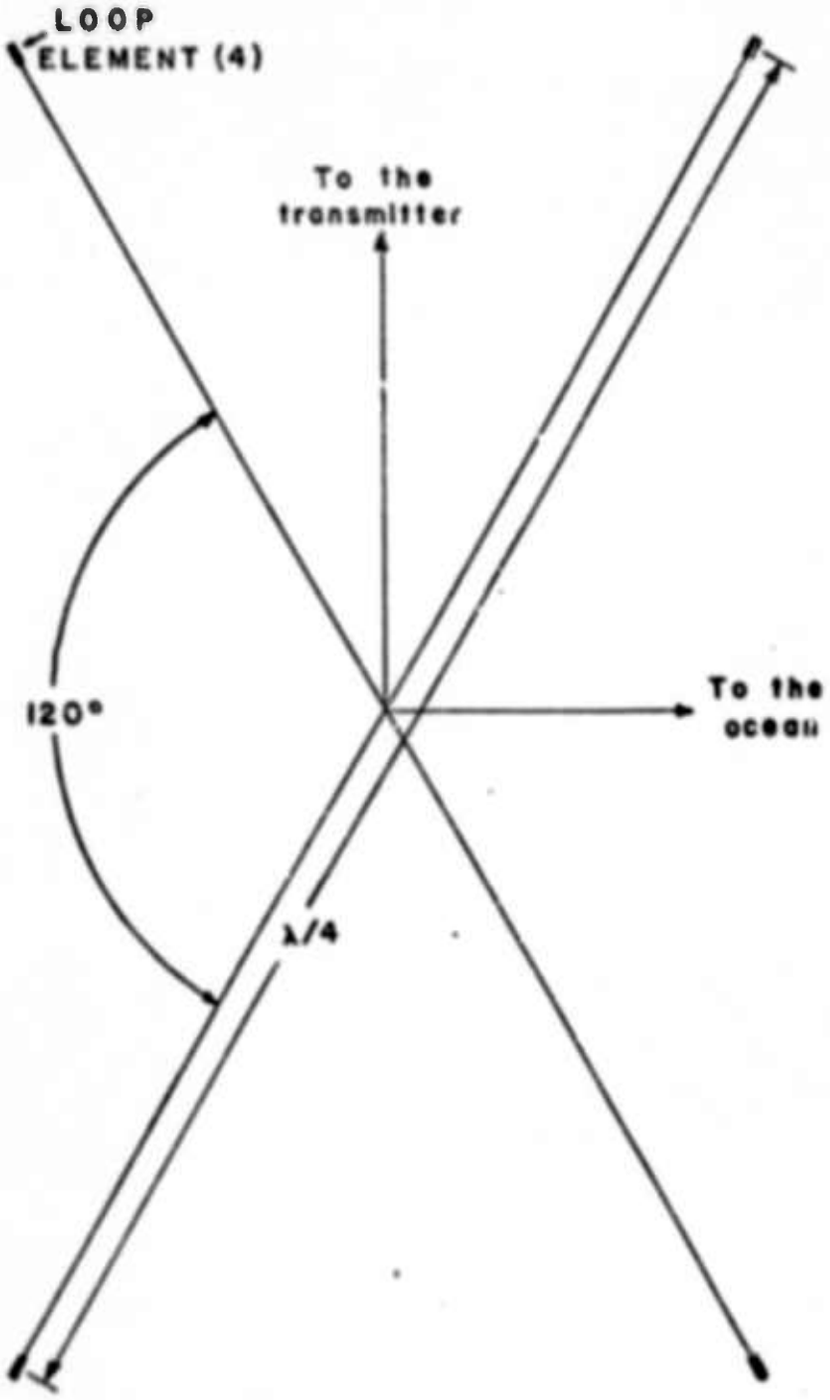

Figure 1. Four element receiving antenna array, and its orientation to the bistatic geometry, used in the Hawaiian bistatic experiment.

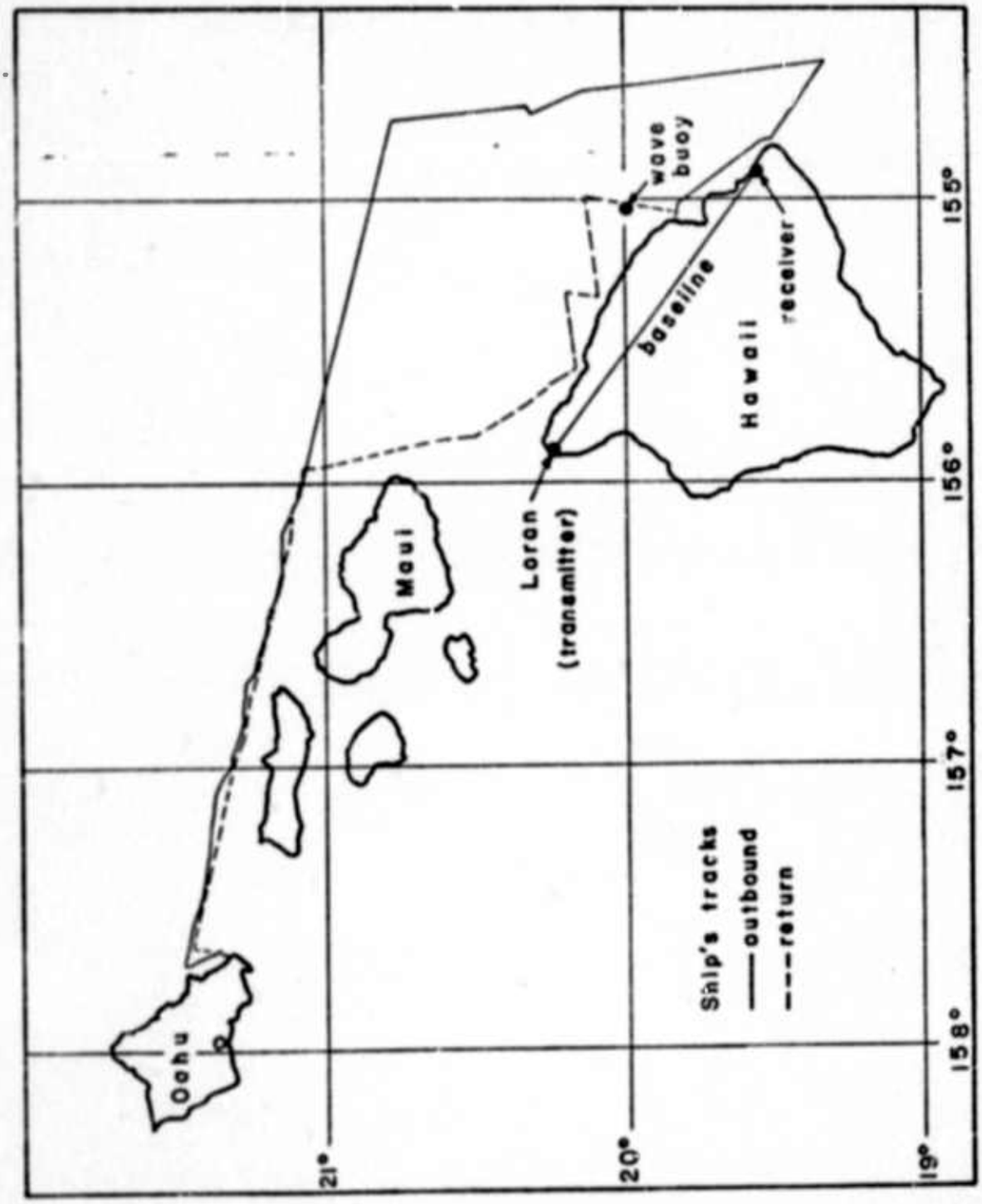

Figure 2. Map of Hawaiian Islands showing location of experiment, and ship tracks over which LORAN field strength measurements were made.

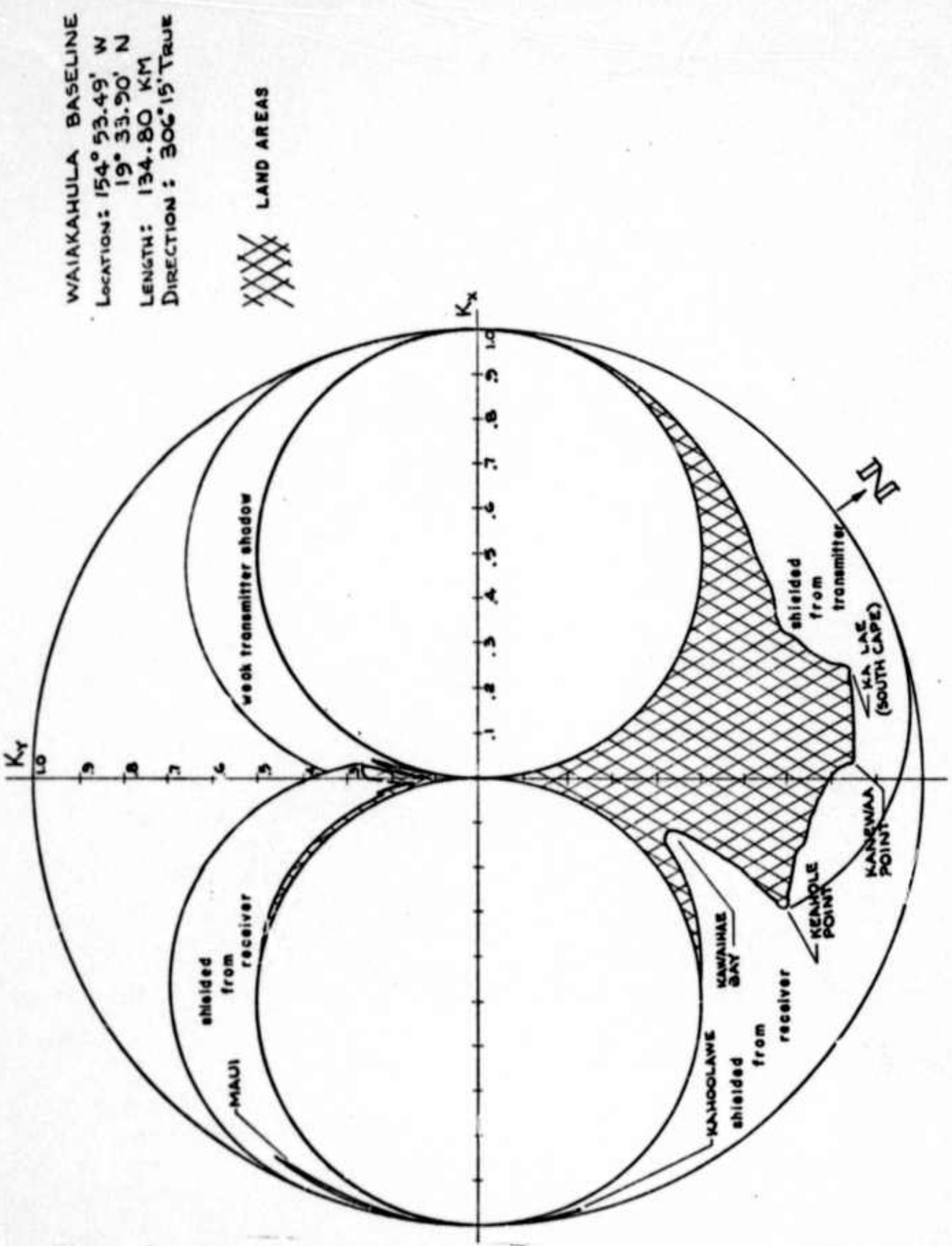

Figure 3. The Hawaiian bistatic geometry mapped onto ocean wave-number space showing regions occupied by land, and regions where the radio signal is shielded by topography. No observations can exist in the figure eight region in the center, observable waves must have a wave number vector lying on the clear area near + K_y

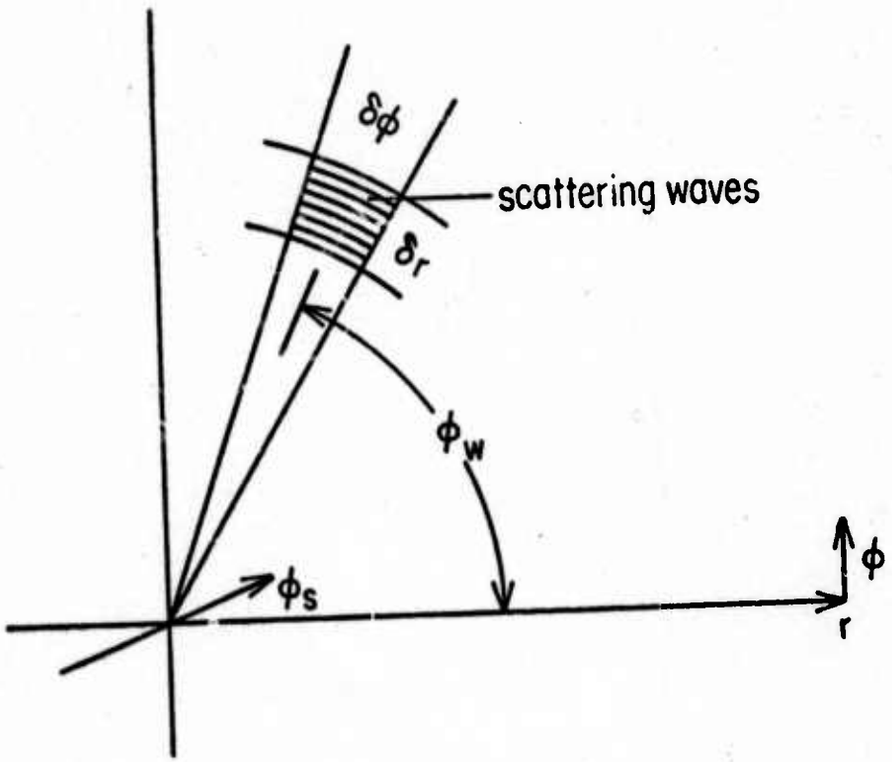

Figure 4. Geometry for synthetic aperture measurements. Receiver moves towards ϕ_s with velocity v. This motion synthesizes an antenna having a resolution $\delta\phi$.

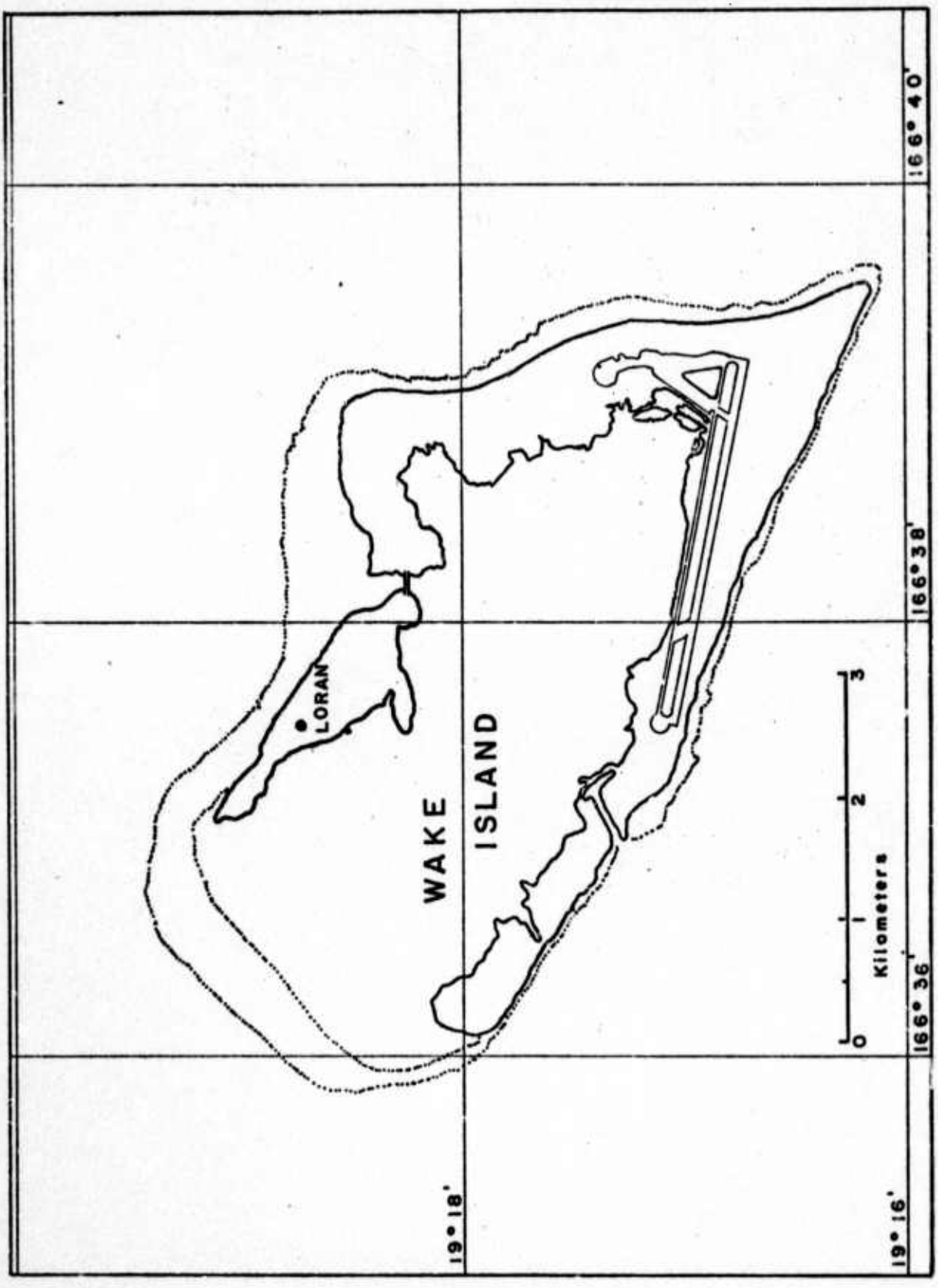

Figure 5. Wake Island. The taxiway to the north of the main runway, and the parking areas to the east of this runway, were used in the synthetic aperture experiment.

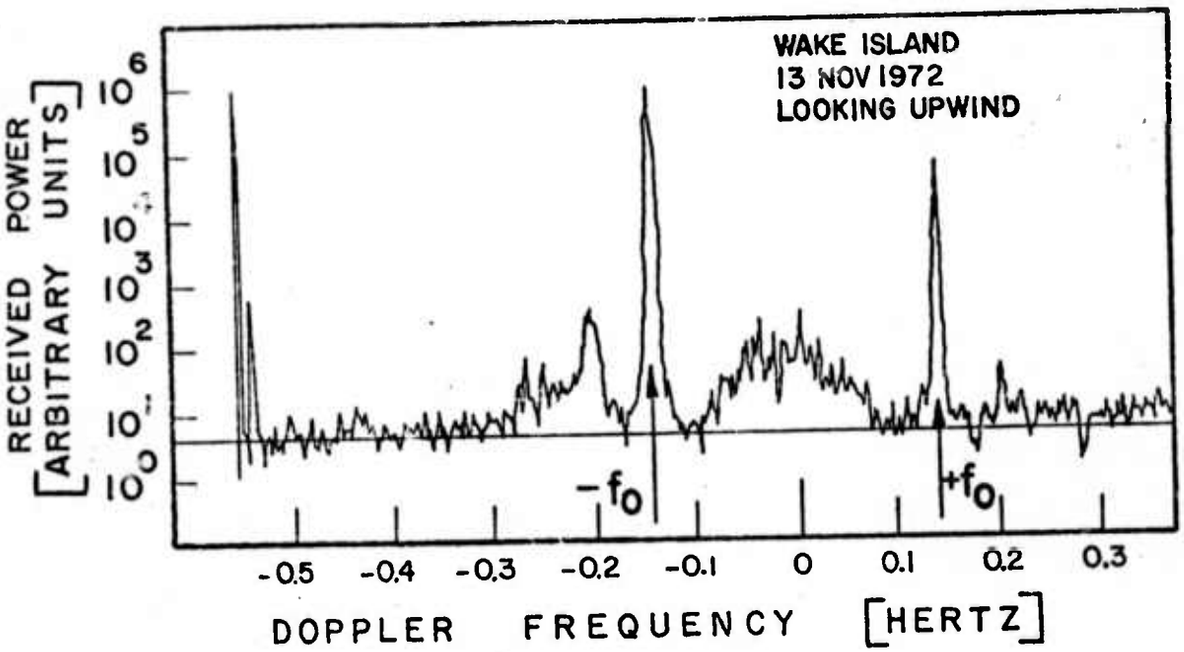

Figure 6. Typical Doppler spectrum of 1.85 MHz signals backscattered from the sea near Wake Island. Spectrum shows two clean lines due to Bragg scattered signals at $\pm f_o$, plus sidebands due to higher-order scattering at 0 and -0.22 Hz. Peak at -0.55 Hz is due to system noise.

Part III

ADVANCED STUDIES IN NEARSHORE ENGINEERING

Principal Investigator
Dr. Douglas L. Inman
Phone (714) 453-2000, Extension 1175

ADVANCED OCEAN ENGINEERING LABORATORY

Sponsored by

ADVANCED RESEARCH PROJECTS AGENCY

ADVANCED ENGINEERING DIVISION

ONR Contract N00014-69-A-0200-6012

Part III

ADVANCED STUDIES IN NEARSHORE ENGINEERING

Table of Contents

List of Tables

List of Figures

I. Project Summary

Research during the past two contract years has been directed towards understanding the mechanics of motion over phase dependent roughness elements and the limits to their application in controlling the transport of sand. The mechanics of the process is based on the differential vortex formation over the faces of asymmetrical "ripple like" bottom roughness elements. The differential vortex formation leads to differing amounts of sand suspension on the respective faces of the roughness elements and hence a preferred direction of sand transport.

During the first half of this contract year, the broad limits of applicability of this process were ascertained, and then the reasons for these limits were investigated. The studies showed that the roughness elements were most effective for steepnesses of 0.15, where steepness is defined as the height of the roughness element divided by the wavelength of the roughness. This is the same value of steepness for sand ripples found in nature. For elements with steepnesses greater than 0.15 the vortex over the steep side of the form was destroyed and its ability to suspend sediment lessened. The vortex breakdown leads to flow conditions where sediment transport was no longer in the required direction. These studies were carried out in a laboratory wave channel, using the flow visualization techniques of dye injection and hydrogen bubble formation along a fine wire. In order to better study the nature of the differential vortex formation, vortices over symmetrical wave-generated ripples were also studied, using the two flow visualization techniques. Once the design criteria for the phase dependent roughness elements were ascertained from the laboratory work, prototype size elements were constructed and placed in the nearshore zone to test the applicability of the method in the marine environment. The results of these tests were encouraging and showed that the method was indeed operational on a small scale.

Efforts during the last half of this contract year have been centered on developing a workable system to be used in a large scale sediment transport control problem. In addition, work has been carried out to understand the amount of wave energy loss brought about by the generation of vortices over symmetrical ripples.

II. Present Research

In developing a workable field array of phase dependent roughness elements, one of the principal problems has

been the development of a method of installing the array of elements and maintaining their location once they have been installed. The earlier small scale testing in the nearshore zone utilized elements constructed out of concrete. The design of the field elements calls for an array 3 meters wide in the on-offshore direction and of one piece construction to prevent tilting of the elements with respect to one another. Accurate placement of the elements is also required. Since concrete forms of this size would weigh approximately 2000 pounds, a barge or other large vessel would be needed for emplacement.

For initial field tests the arrays were fabricated out of molded fiberglass. These forms could be emplaced with a small craft, and their location supervised by divers. Once in the proper location and alignment, the forms could be weighted or anchored to the bottom to prevent any further motion.

In general high waves are associated with lower slopes while the steepest beach slopes are associated with gentle waves. The flatest beach profiles and those most inducive to erosion are associated with high, short period waves; particularly when these waves are accompanied by strong onshore winds.

Thus, the basic placement and design criteria for arrays of phase dependent roughness elements that are to maintain sand on beaches subject to erosion and seasonal changes are: (1) the arrays should be placed offshore from the beach at the depth where the seasonal changes in beach profile show a "nodal point"; i.e., where the profile maintains a nearly constant depth, with greater changes seaward and landward; and (2) the phase dependent elements should be designed to provide an onshore transport during periods of high waves.

Using these criterion, the projected winter wave climate for the La Jolla area (Lewicki, 1968) and the design criteria from the laboratory tests, three different arrays of roughness elements were constructed. Applying the design criteria to this data, the conclusion is reached that the beach will start eroding when seven second waves and do so for the shorter period waves also. Using the orbital diameters thus arrived at, and calculating the value of the expression $d_o/2\lambda$ which is a controlling factor for phase dependent roughness elements, the wavelengths of the roughness elements can be set at 60 cm. This wavelength yields a value for $d_o/2\lambda$ of 2.1 for the seven second, 2.5 m high waves which is in the range of phase dependent roughness validity. Three elements were constructed. The different wavelength elements

bracket the expected values for phase dependent transport in order to verify the laboratory tests, and thus finalize the design criteria for the most efficient movement of sediment.

The dimensions of these elements are given in Table 1, while Figure 1 shows the construction details. Note that the forms were constructed in two pieces, so that the bottom tray could be emplaced, and weighted, before the top or phase dependent section of the forms was installed.

The middle size element was installed in the nearshore environment and weighted with sand. Though the elements seemed to be controlling the movement of sand as they had in the earlier testing with the concrete elements, it became evident that scouring and subsequent burial of the elements would negate their influence after only a short period in place. To overcome this difficulty, a Carthage Mills, Inc. product, "Filter-X" was emplaced under the roughness element forms. This material is designed to be permeable to water in order to prevent a buildup in pressure head under the filter, while the mesh must be small enough to prevent the underlying sediment from being eroded (Barrett, 1966). An improved method of emplanting the elements and the filter cloth is being worked on. The filter cloth does seem to stop the scouring at the edges of the roughness elements, however, end effects from the edges of the filter cloth have yet to be overcome.

An analytical expression for the amount of energy bound up in the vortices generated in the lee of symmetrical ripples has been developed. In addition, preliminary results indicate that the vortices may be represented by a simple potential plus forced vortex model. Agreement between the model and the measured values of the velocity structure in the wave generated vortices is good. In addition the vortex energy seems to be a constant percentage of the wave energy loss due to bottom effects as measured by several other researchers. This agreement holds over a range of 3 orders of magnitude.

Future work will entail the finalizing of methods for installing and maintaining the phase dependent roughness elements in the nearshore zone and completing the work on the structure and energy in the wave generated vortex field.

III. References

Barrett, R. J., 1966, "Use of plastic filters in coastal structures", *Proc. Tenth Conference Coastal Engineering, Tokyo, Japan.*

Inman, D. L. and R. A. Bagnold, 1963, "Littoral processes" in *The Sea: Ideas and Observations*, vol. 3, The Earth Beneath the Sea (ed M. N. Hill) Interscience Publ., p. 529-53.

Lewicki, A., 1968, "Wave study for Scripps Island Site", *Marine Advisors Inc.* La Jolla, California, 29 pp.

Table 1. Dimensions of the prototype roughness elements and test arrays. The asymmetry, horizontal projection of steep face divided by the wavelength was 0.25 in each case

ARRAY				ROUGHNESS ELEMENT		
TYPE	WIDTH	LENGTH	NUMBER OF ELEMENTS	HEIGHT η	WAVELENGTH λ	STEEPNESS η/λ
A	2.0 m	3.0 m	15	3.0 cm	20 cm	0.15
B	"	3.2 m	8	6.0 cm	40 cm	"
C	"	3.0 m	5	9.0 cm	60 cm	"

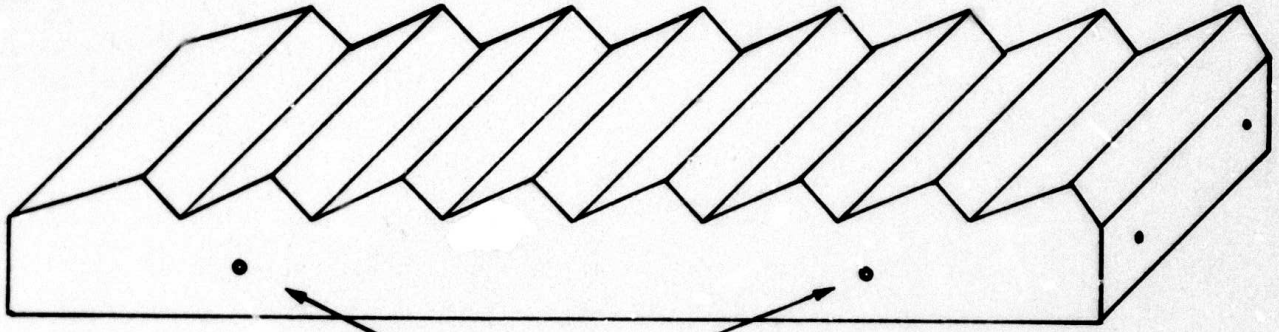
FASTENERS

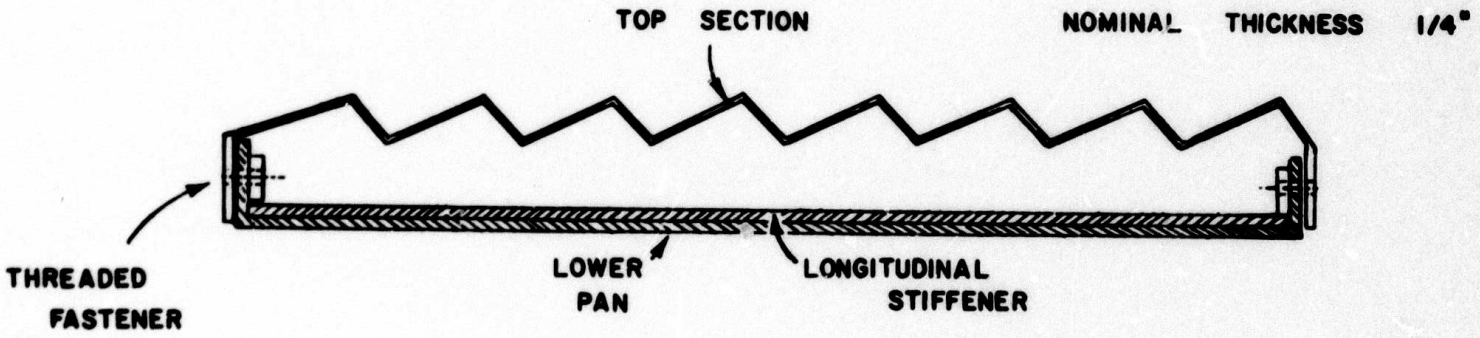
TOP SECTION
NOMINAL THICKNESS 1/4"
THREADED FASTENER
LOWER PAN
LONGITUDINAL STIFFENER

73-13-9

Part IV

WAVE BREAKING IN DEEP WATER

Co-Principal Investigators
Dr. W. G. Van Dorn
Phone (714) 453-2000, Extension 1179
Dr. R. E. Davis
Phone (714) 453-2000, Extension 1301

ADVANCED OCEAN ENGINEERING LABORATORY

Sponsored by

ADVANCED RESEARCH PROJECTS AGENCY

ADVANCED ENGINEERING DIVISION

ONR Contract N00014-69-A-0200-6012

Part IV

WAVE BREAKING IN DEEP WATER

Table of Contents

List of Figures

I. Project Summary

This report summarizes the results of the second six months of our projected two-year laboratory and field investigation of the factors controlling the breaking of mixed-frequency wave systems in deep water, such as occur under storm conditions in the open sea.

During this period, we have completed three sets of experiments in the 8' x 8' x 150' wave tank, in which transient series of periodic waves were squeezed laterally to the breaking point in an 80' convergent section. Because the wave generator was tape-controlled, each wave series could be reproduced arbitrarily, so that consecutive measurements of elevation, pressure, and the orthogonal components of fluid velocity could be conducted at a number of stations along the convergence, and also at a number of depths beneath the free surface at any station. All data were digitally recorded and stored on magnetic tape for computer processing. Most of these data have now been analyzed, and some early results are included herein.

During the next six months, we anticipate continuing the convergent-breaking experiments to fill in some blank spots. We will then remove the convergence and conduct similar measurements among waves that are caused to break as a result of tape-controlled constructive interference, with- and without-wind. Such coincident breaking is considered to be a principal factor limiting sea state under storm conditions.

II. Technical Report

1. Convergent Breaking

Before looking into coincident breaking of multiple-frequency wave systems, it was thought necessary to understand the breaking characteristics of purely periodic waves in deep water, for which there exist some approximate solutions. Subcritical periodic waves can be induced to break by squeezing them laterally in a convergent channel. Lateral convergence imposes certain experimental constraints: introduction of lateral oscillations limits experiments to wavelengths longer than about 80% of the largest width of the convergence (R. Stewart's thesis); distributed reflectance must be considered in the wave energy budget; and the convergence must be again diverged to avoid a strong terminal impedance mismatch, and consequent standing wave production within the convergence. After some preliminary modeling in our smaller wave channel, the final convergent barrier in the 8' x 8' x 150' channel is

shown in Fig. 1, together with the coordinate system to which all measurements are referred. The distributed reflectance was determined for each wave frequency by cross-correlating simultaneous surface elevation records taken by quarter-wavelength apart. It was found to increase from 1-2% to 6-8% between the generator and the breaking point, increasing with frequency.

Because the first few waves in a periodic wave train initiated from rest are strongly dispersive, and because it was found impossible to completely eliminate terminal reflections, we (Fig. 2) resorted to truncated, amplitude-modulated wave trains, defined by variations of the relationship:

$$\delta = \cos wt \cdot \tanh\left(wt/N + \frac{9\pi}{4N}\right);$$

N = 14 for .5 Hz
N = 30 for .73 Hz
N = 24 for .66 Hz

which were computer-generated, and recorded on FM tape for recurrent playback. Fig. 2 is a computer printout of the generator displacement traces, indicating the nature of the input functions for frequencies of 0.50, 0.66, and 0.73 Hz. Fig. 3 shows a typical data record sample at .73 Hz. Although digital data were recorded at the rate of 100/sec/channel for all waves of a sequence, analysis was concentrated on the 5th or 6th crest. By this time the waves have reached peak amplitude, but the earliest terminal reflections have not yet returned to the breaking point. The breaking point can be positioned, within limits, along the convergence by slight amplifier gain adjustments.

2. Data and Procedures (see Ref. 1 for instrument description)

Each data run consisted of the generation of a transient train of waves as described above, during which the following variables were recorded at 0.01 sec intervals for 10.24 sec:

a) surface elevation at two cross-channel and two long-channel positions;
b) forward and vertical components of fluid velocity at depth Z in mid-channel;
c) subsurface pressure at lower end of reference wave staff, and on bottom near wave generator. The latter sensor is fixed, and indicates whether consecutive runs are identical.

After each run, the elevation of the velocity probes was altered, or the sensor cart rolled to a new station. All told, a total of ~270 data runs were completed, roughly divided

among three wave frequencies, ∿9 elevations, and 10 stations. These data are sufficient to permit consistent reconstruction of the vector velocity and acceleration fields within individual waves at all stages of growth up to the point of intense breaking. The rapid response (>10 kHz) of the hot-film velocity probes also make possible future increases in the data sampling rate as high as 1000/sec, such that very rapid changes can be defined. Fig. 3 is a revised analogue record for a typical data sequence.

3. Preliminary Results

a) Wave profiles: Figs. 4a, b & c show consecutive time histories of surface elevation, as a function of distance from the wave generator, for our three reference frequencies. The water depth was adjusted at 0.66 and 0.73 Hz to give the same depth/wavelength ratio. The depth at 0.50 Hz is the greatest possible without altering the input amplitude. The latter waves are not strictly deep-water, in the usual sense, but were still found to approach limit breaking conditions in much the same manner as the higher frequency waves (Ref. 2).

In all cases, amplitude, wavelength, and phase velocity increase smoothly toward the breaking point, as indicated by the bottom profiles. All waves remain fairly symmetrical until just before breaking. The breaking crest angles and steepnesses were observed to be fiarly close to the theoretical Stokes and Michell limits of 120° and 0.143, respectively (Refs. 3 & 4).

b) Particle velocities: (Fig. 5) The maximum particle velocities in the .73 Hz and .66 Hz waves approach the infinitesmal wave phase velocity ($gT/2\pi$). The .5 Hz wave does not have such high velocities, however, and was probably measured too soon before breaking. The highest velocities of the wave are contained in a jet just under the crest of the wave. This jet appears to grow rapidly just before breaking; it is most prominent in the .66 Hz wave but also can be seen in the .73 Hz wave.

c) Particle accelerations: (Fig. 6) Particle accelerations exceed 1/2 g at breaking for both .73 Hz and .66 Hz; accelerations were again much smaller in the .5 Hz wave. The expected particle acceleration is 1/2 g from the theory for the limiting Stokes' wave (Ref. 5). The highest observed particle accelerations occurred in the region of the velocity jet; in fact,

there appears to be an associated acceleration 'jet' in both the .73 Hz and .66 Hz waves.

d) Phase velocities: Rough estimates at present of phase velocity have been made only from the analogue records. These generally exceed the theoretical small-amplitude velocities by 10-20%. More accurate phase velocities can be obtained from cross spectra between two adjacent wave staffs, but have not yet been calculated.

e) Energy budget: We have not yet attempted to compute energy. However, using the data we have now, it will be possible to compare the kinetic energy of the limiting wave with its potential energy. A complete analysis can also let us compare the real rate of energy accretion with that expected due to lateral convergence.

4. Preliminary Conclusions

Our present results are extremely encouraging. The velocity measurements are the first ever completed in sufficient detail to permit accelerative calculations anywhere within the flow field. The fact that peak horizontal accelerations were observed to substantially exceed gravity, and occurred somewhat below the surface, provides some insight into the often-reported breaking jet. The fact that pre-breaking velocities are reasonably in accord with those for limiting Stokes' waves, gives some hope of applying basic theory to coincident interactions between waves, as projected in later experiments.

III. Future Plans

1. Laboratory Phase

Our experimental schedule is inescapably related to other demands for the large wind-wave channel. We have requested two months of channel time for 1973, the first in February, and the latter in April-May. During the first month, we shall continue working with convergent waves, at high data rates, and also exploring the influence of wind and surface tension. This program would have continued last Fall, except for competitive programs. This unfortunately required that we remove the convergent barrier--a task requiring 16 man days--and will probably require somewhat longer to reinstall.

Our late spring experiments will be directed toward breaking due to coincident interactions between waves of different

frequencies. It is probably optimistic to expect to complete the latter experiments within one month of channel time, and we anticipate the need for an additional month of experiments during the summer.

We are making good progress in an entirely new and fertile field, and are extremely encouraged by our results to date.

2. Field Phase

We earlier anticipated the possibility of making some correlative field observations of velocity and elevation within breaking waves from some suitable platform, such as R/P FLIP. At present, this does not appear to be realistic within time and budget limits for calendar 1973. FLIP's schedule does not put her within a representative storm wave area within the next year. While the desired observations could be made from any of a number of drilling rigs in the North Sea, or Alaska, we have neither funds nor adequate time to prepare for an expedition of this magnitude. However, we will devote the balance of experimental effort late this year to evaluating probe performance in sea water from the end of Scripps Pier, and to preparing a suitable field experiment for completion in 1974.

IV. Bibliography

1. Van Dorn, W. G. and R. E. Davis, Wave Breaking in Deep Water, AOEL, Tech. Progress Report, June 30, 1972.

2. Miche, M. (1954) Undulatory Movements of the Sea in Constant or Decreasing Depth, Univ. of Calif. at Berkeley Inst. of Eng. Res. Report, Series 3, Issue 363.

3. Stokes, G. G. (1847) "On the theory of Oscillatory Waves," Trans. Cambridge Philosophical Soc., VIII, pp. 441.

4. Michell, J. G. (1893) "On the Highest Waves in Water," Philosophical Magazine, Vol. 36, No. 5, pp. 430-435.

5. Longuet-Higgins (1963) "The Generation of Capillary Waves by Steep Gravity Waves," JFM, Vol. 16, pp. 138-159.

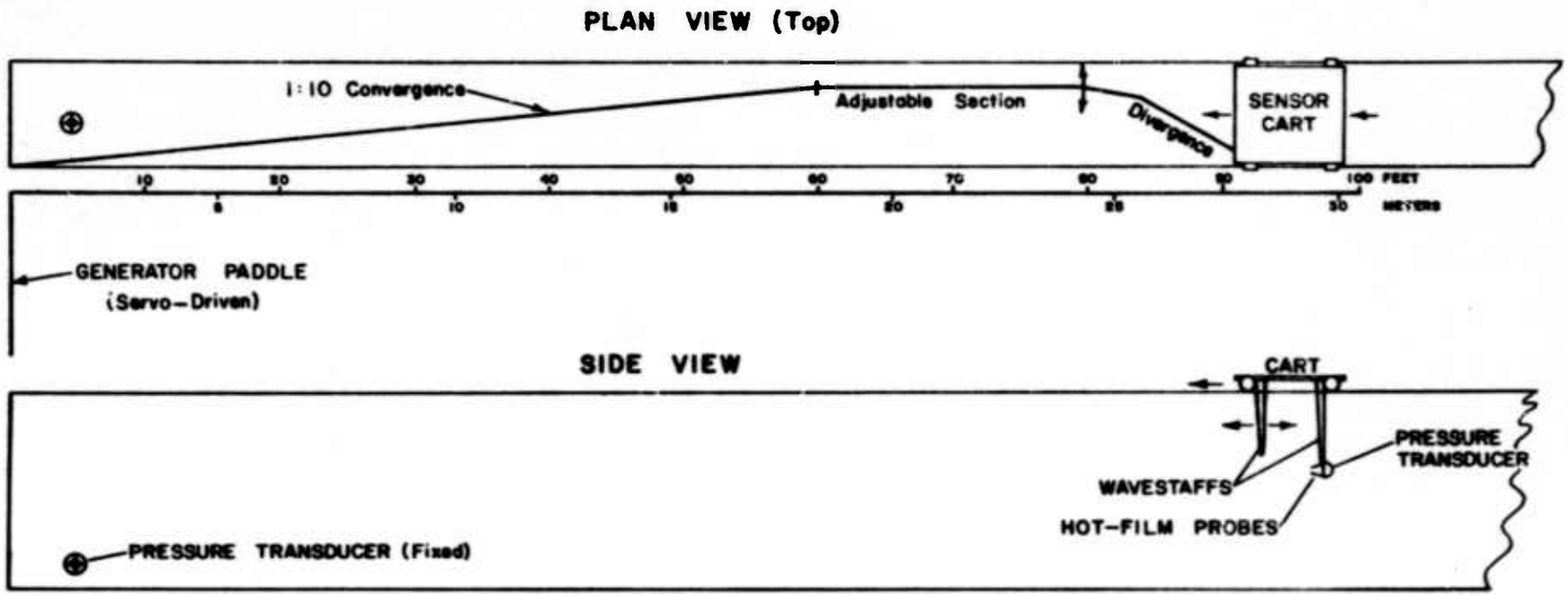

Figure 1. Schematic drawing of 8' x 8' x 150' wind wave channel, showing convergent barrier and instrument sensor cart.

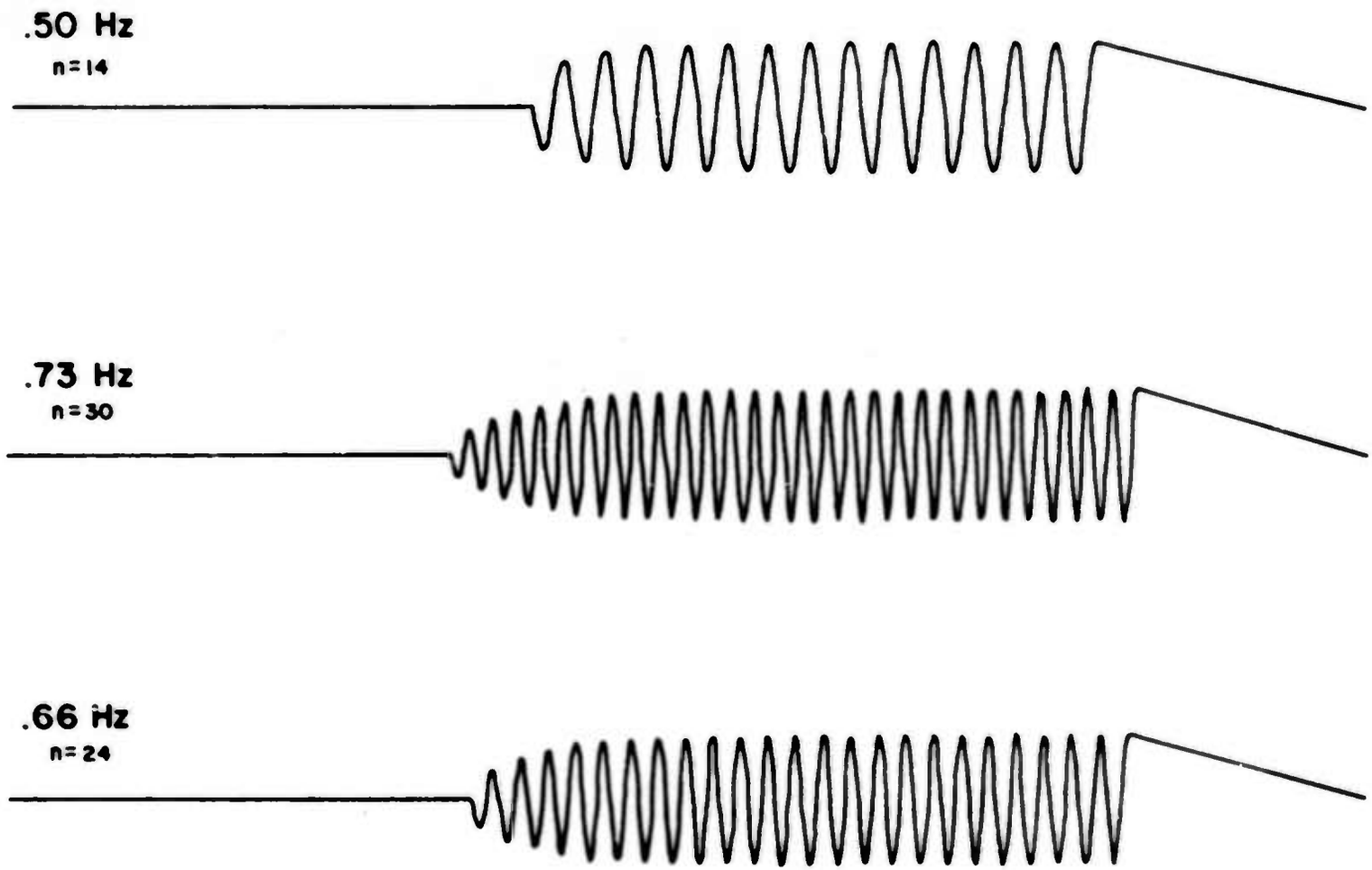

Figure 2. These are the voltage inputs to the paddle servomechanism. The displacement of the paddle is proportional to the voltage. The analytic expression used to compute this wave form is

$$\delta = \cos wt \cdot \tanh (wt/n + 9/4n)$$

n = empirically determined to control breaking point.

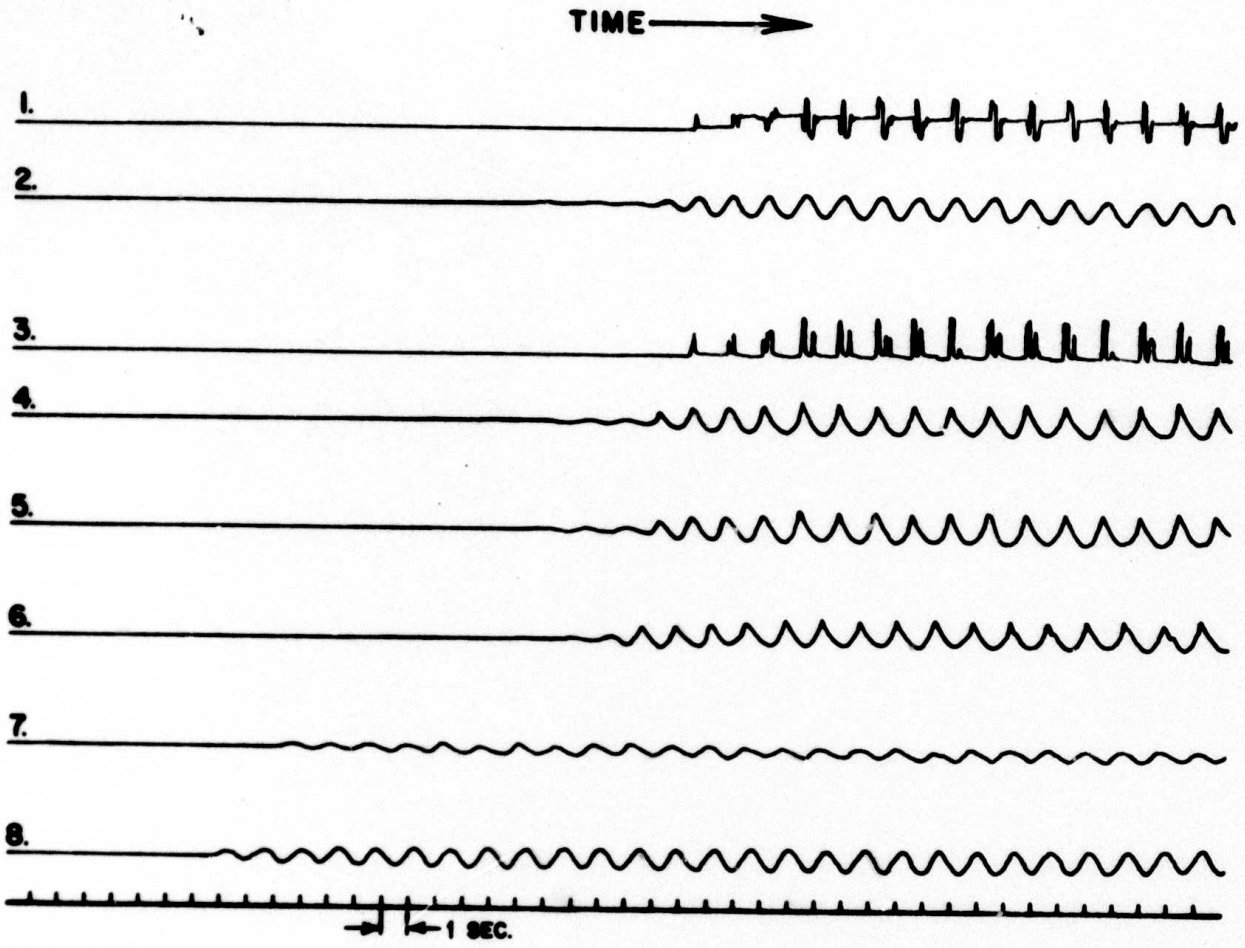

Figure 3. This is a sample record from the Statos chart recorder. Time runs from right to left in each record. From top to bottom the signals are from: 1. the hot-film probe (top), 2. the pressure transducer at wavestaff #2 position, 3. the hot-film probe (bottom), 4. wavestaff #3, 5. wavestaff #1, 6. wavestaff #2, 7. the pressure transducer near the paddle, 8. the paddle arm motion transducer. This record was taken about 6 1/2 cm below the crest and about 5 cm before the point of breaking of a .73 hz wave.

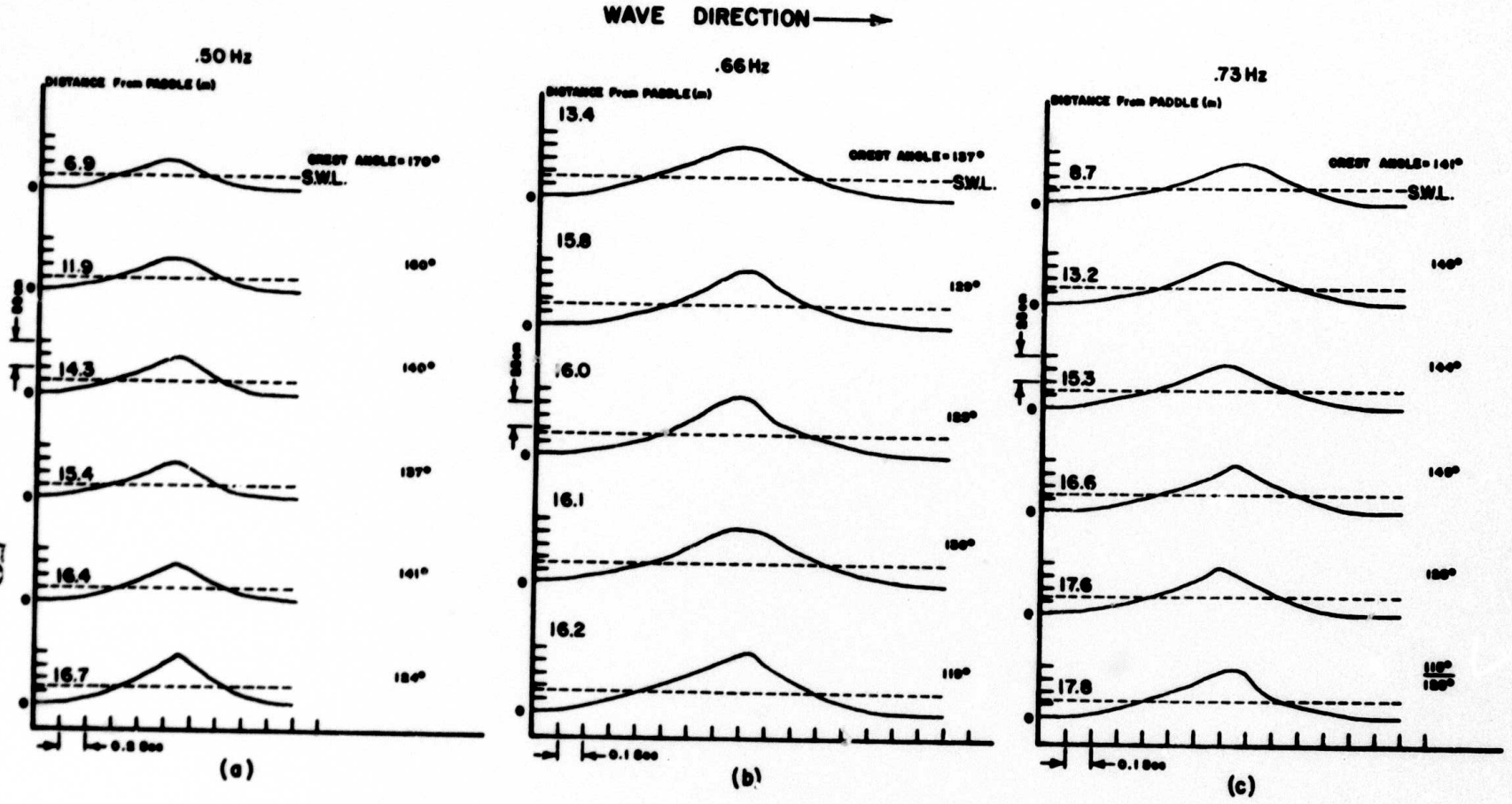

Figure 4. These figures show the changes in the profiles of the waves of different frequencies as they approach breaking; time progresses from top to bottom. Note the sudden asymmetry at breaking, and note how the crest angle progressively becomes smaller up to the moment of break. The limiting angle is 120°.

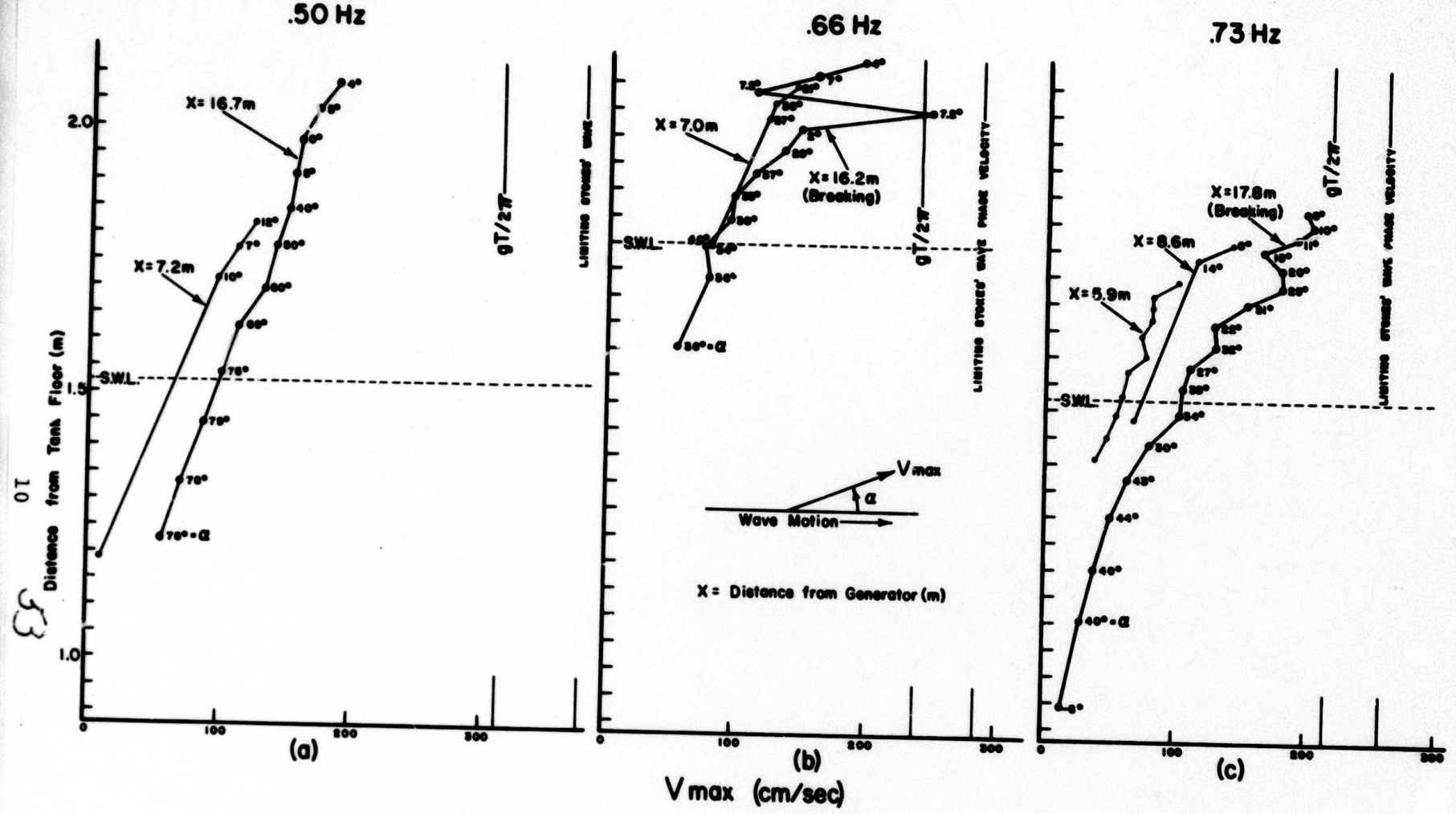

Figure 5. These are vertical profiles of velocity maxima taken at different positions in the tank. The .66 hz wave shows a very strong jet 10 cm below the crest, the .73 hz wave shows a jet just 2.5 cm below the crest, and the .5 hz wave shows no jet at all. The stars and triangles mark measurements taken far before breaking, while the squares indicate measurements at breaking is the rapid growth of the subcrestal jet. We believe measurements of the .5 hz wave were taken too soon before breaking; we will attempt to rectify this during the next experimental session.

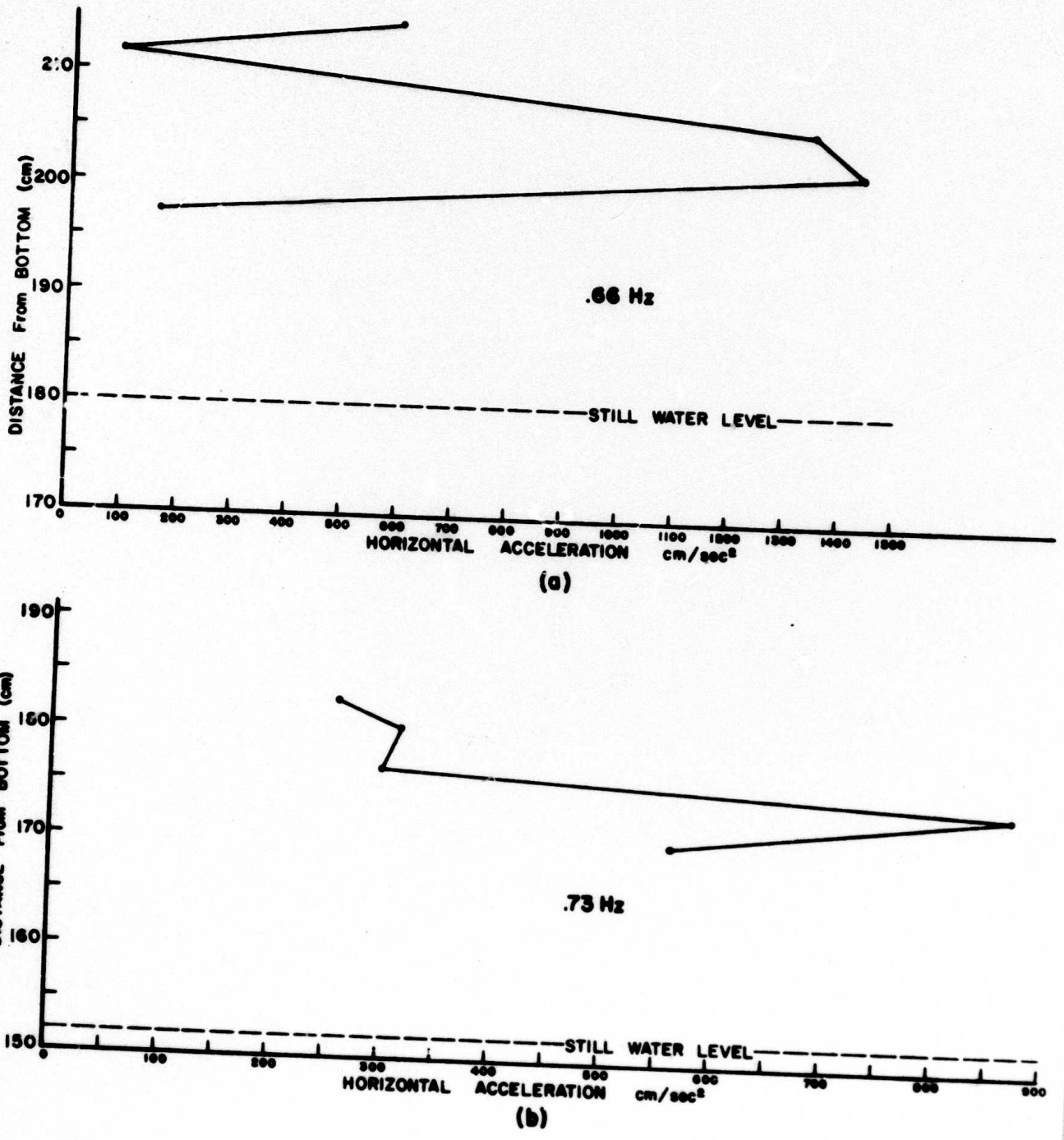

Figure 6. Lagrangian accelerations in the waves at breaking point profiled against depth. These are accelerations of horizontal velocity. Note how closely the peaks in acceleration and in velocity match. It is of particular interest to see such a high acceleration measured; the theoretical value at breaking is 1/2 g.